QRPA based calculations for neutrino scattering and electroweak excitations of nuclei.

Arturo R. Samana
in collaboration with
Francisco Krmpotic, Alejandro Mariano, Cesar Barbero – UNLP -Argentina
Carlos A. Bertulani -Texas A&M University – Commerce-USA
Nils Paar – University of Zagreb – Croatia

08/11/2015

(NUCFACT2015) – Rio de Janeiro- Br - 2015

Outline

- Motivation

Neutrino physics and Nuclear Structure.

- Weak-Nuclear interaction

Formalism

Nuclear Models

SM, RPA, QRPA, PQRPA, RQRPA

- Results on 12C, 56Fe and systematic

calculations

- Summary

Motivation

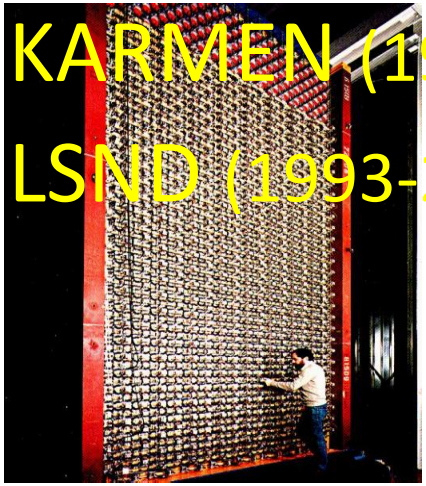

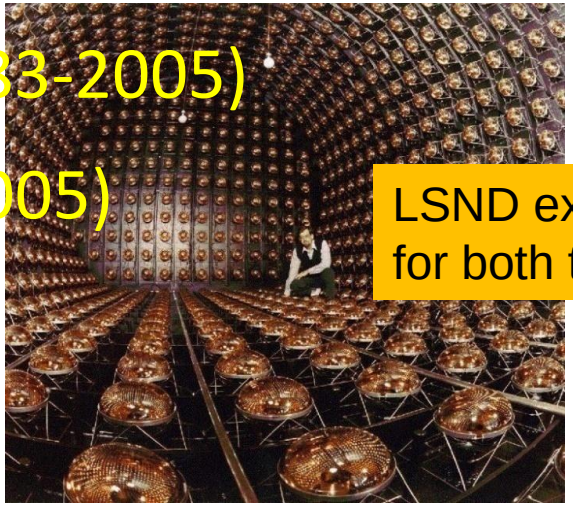

KARMEN, no oscillation signal

LSND experiment observes excesses of events for both the $\bar{\nu}_\mu \rightarrow \bar{\nu}_e$ and $\nu_\mu \rightarrow \nu_e$ oscillation.

$$\bar{\sigma}(J_f) = \int n(E_\nu)\sigma(E_\nu, J_f)dE_\nu$$

Table 1

Calculated and experimental flux-averaged exclusive $\bar{\sigma}^{\text{exc}}_{e,\mu}$, and inclusive $\bar{\sigma}^{\text{inc}}_{\mu}$ cross-section for the $^{12}\text{C}(\nu_e, e^-)^{12}\text{N}$ DAR reaction (in units of 10^{-42} cm^2) and for the $^{12}\text{C}(\nu_\mu, \mu^-)^{12}\text{N}$ DIF reaction (in units of 10^{-40} cm^2). The CRPA calculations [15] were used in the first LSND analysis on the 1993–1995 data sample [2], and the SM calculations from Ref. [16] in the second LSND oscillation search [3]. The listed PQRPA results correspond to the calculations performed with the relativistic corrections included [17]. One alternative SM result as well as the RPA and QRPA results from Ref. [19] are also shown

	$\bar{\sigma}^{\text{exc}}_{e}$	$\bar{\sigma}^{\text{inc}}_{e}$	$\bar{\sigma}^{\text{exc}}_{\mu}$	$\bar{\sigma}^{\text{inc}}_{\mu}$
Theory				
CRPA [15]	36.0, 38.4	42.3, 44.3	2.48, 3.11	21.1, 22.8
SM [16]	7.9	12.0	0.56	13.8
PQRPA [17]	8.1	18.6	0.59	13.0
SM [19]	8.4	16.4	0.70	21.1
RPA [19]	49.5	55.1	2.09	19.2
QRPA [19]	42.9	52.0	1.97	20.3
Experiment				
Ref. [20]	$9.1 \pm 0.4 \pm 0.9$	$14.8 \pm 0.7 \pm 1.4$		
Ref. [21]			$0.66 \pm 0.1 \pm 0.1$	$12.4 \pm 0.3 \pm 1.8$
Ref. [22]	$8.9 \pm 0.3 \pm 0.9$	$13.2 \pm 0.4 \pm 0.6$		
Ref. [23]			$0.56 \pm 0.08 \pm 0.10$	$10.6 \pm 0.3 \pm 1.8$

A. Samana , F. Krmpotic , A. Mariano,R. Zukanovich Funchal/ Phys. Lett B642(2006)100

Motivation

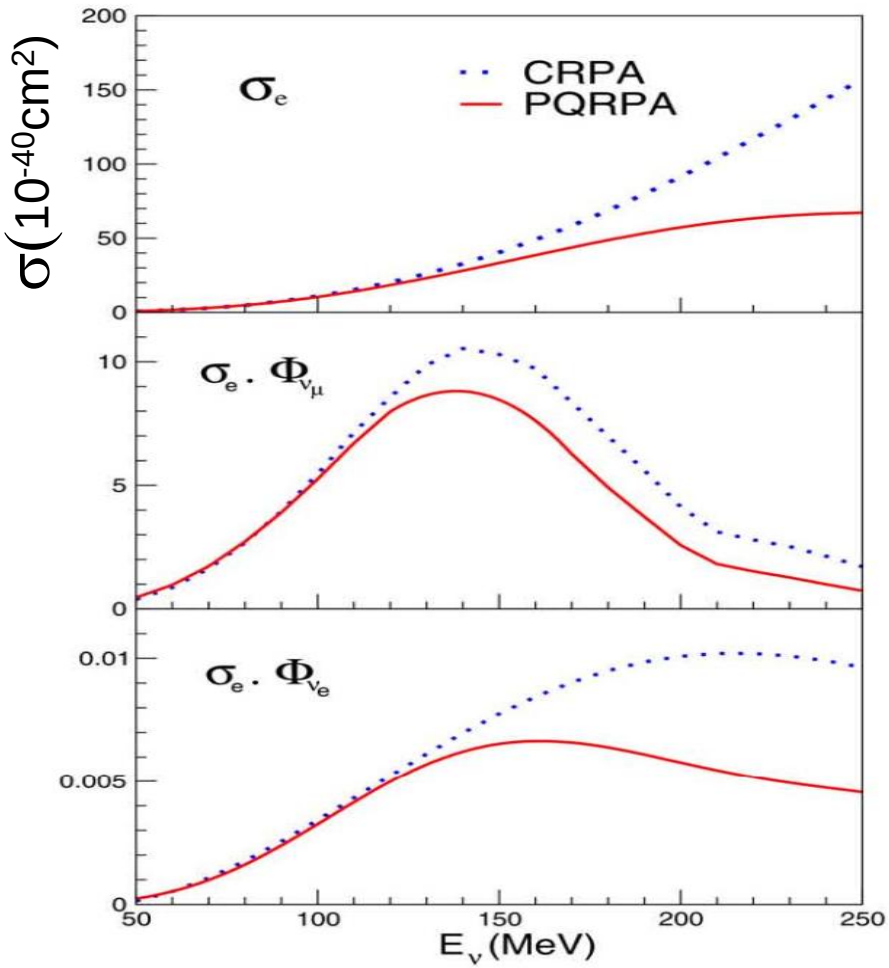

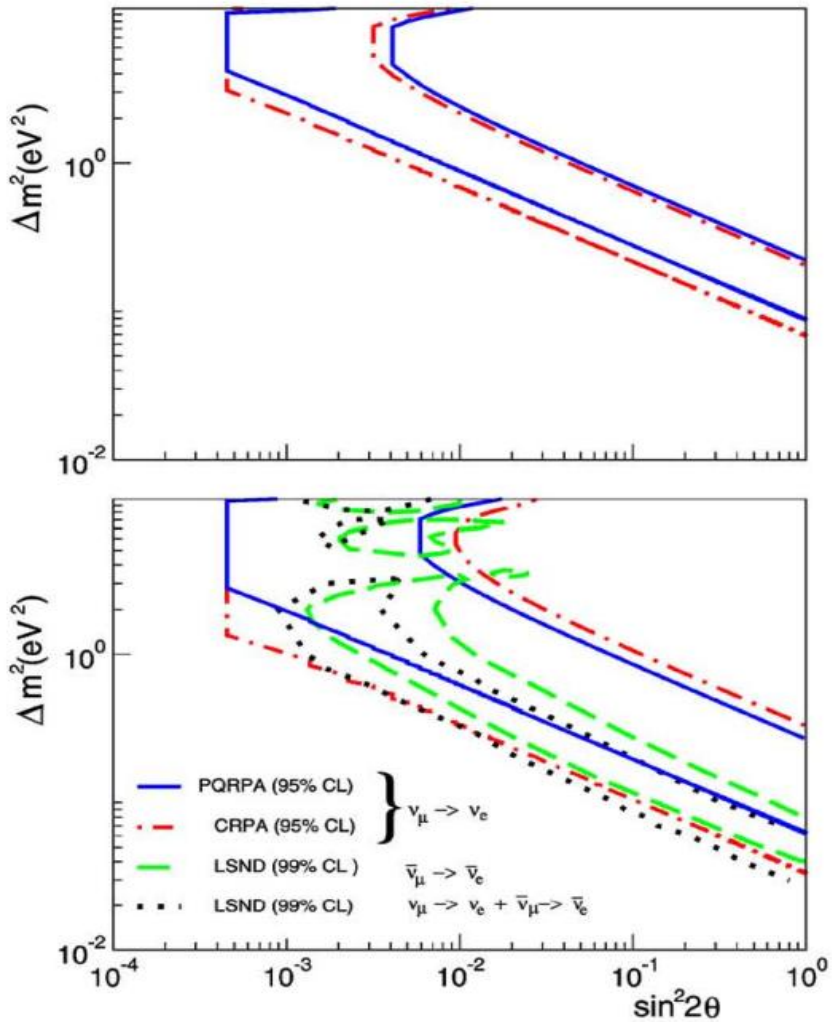

ν-nucleus cross section are important to constrain parameters in neutrino oscillations.

$$\bar{\nu}_\mu \rightarrow \bar{\nu}_e \qquad \nu_\mu \rightarrow \nu_e$$

* Increase probability oscillations.
* Confidence level region is diminished by difference in σ_e between PQRPA and CRPA, PLB (2005) 100

Supernovae Neutrinos – Signal Detection

Number of target nuclei

Neutrino flux

Interaction cross section

Efficiency $\sigma(E_\nu)$

$$N_{ev} = N_t \int_0^\infty F(E_\nu)\cdot\sigma(E_\nu)\cdot\varepsilon(E_\nu)dE_\nu$$

$F(E_\nu)$

SNO

$$\nu_e + d \rightarrow p + p + e^-$$

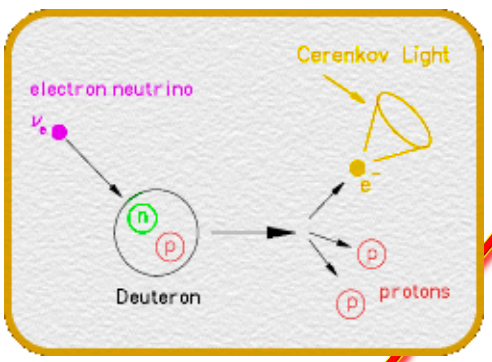

$$\bar{\nu}_e + p \rightarrow n + e^+$$

LVD

Super-K

$$\nu_e + {}^{16}O \rightarrow {}^{16}F + e^-$$

$$\bar{\nu}_e + {}^{16}O \rightarrow {}^{16}N + e^+$$

$$\nu_e + {}^{12}C \rightarrow {}^{12}N + e^-$$

$$\bar{\nu}_e + {}^{12}C \rightarrow {}^{12}B + e^+$$

$$\nu_e + {}^{56}Fe \rightarrow {}^{56}Co + e^-$$

$$\bar{\nu}_e + {}^{56}Fe \rightarrow {}^{56}Mn + e^+$$

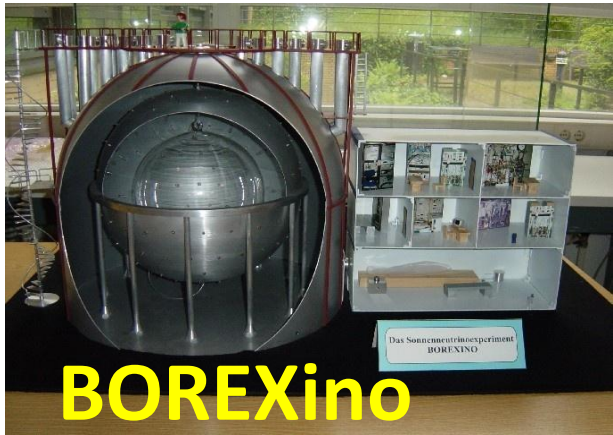

Weak–nuclear interaction

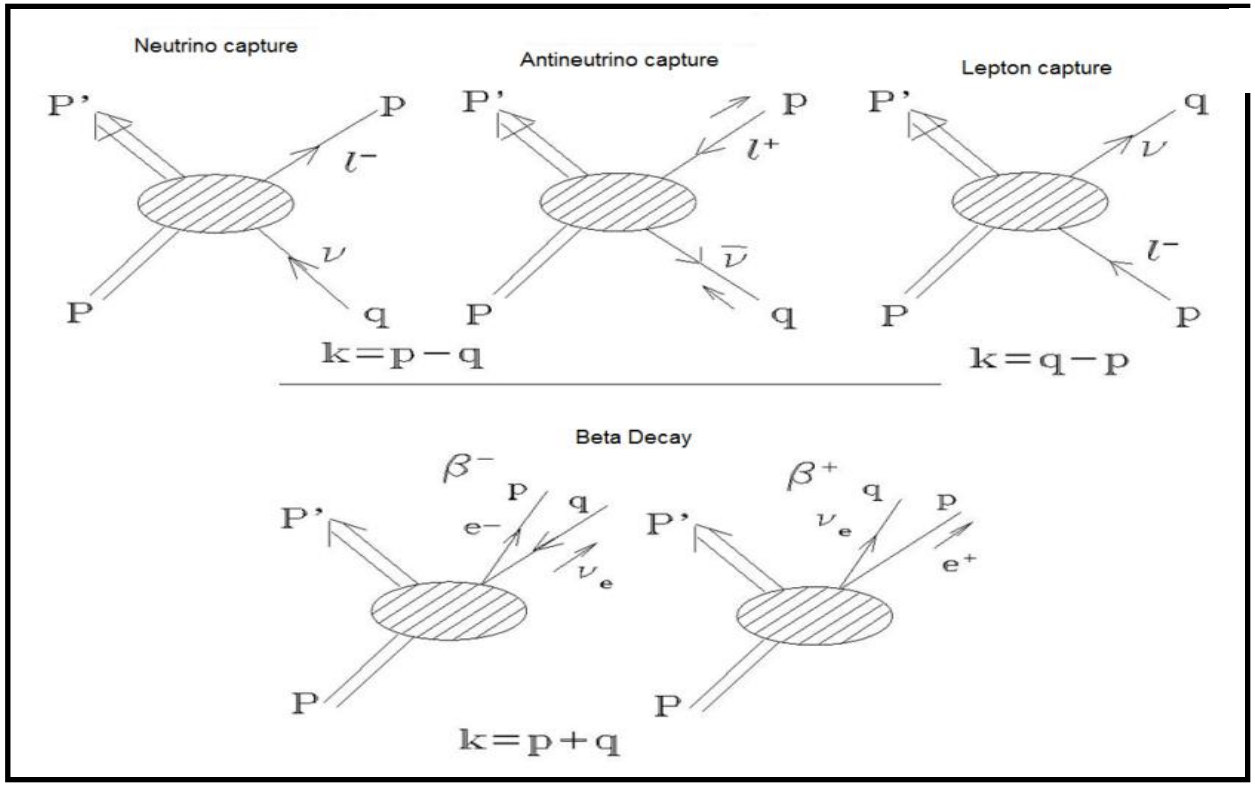

Charged Current

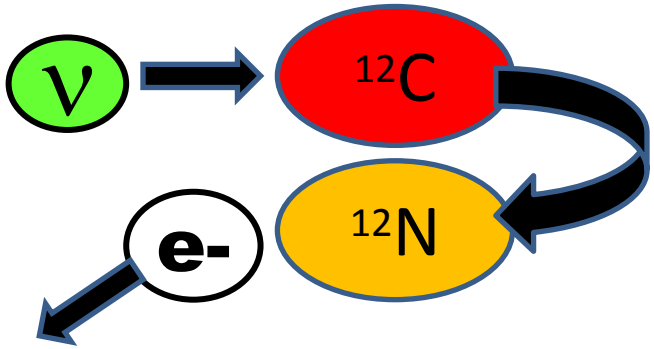

Neutral Current

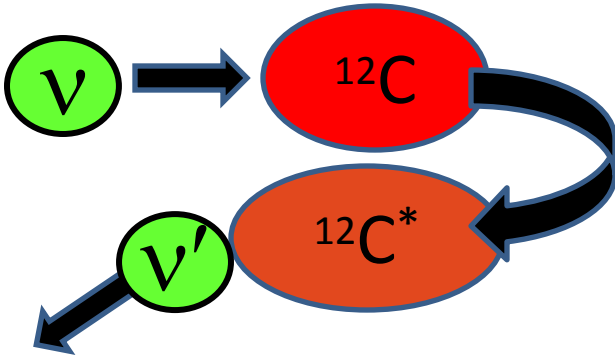

$$\nu_e + A(Z,N) \Rightarrow A^*(Z+1, N-1) + e^-$$

$$\bar{\nu}_e + A(Z,N) \Rightarrow A^*(Z-1, N+1) + e^+$$

(i)O'Connell, Donelly & Walecka, PR6,719 (1972)
(ii) Kuramoto etal. NPA 512, 711 (1990)
(iii) Luyten etal. NP41,236 (1963)
(iv) Krmpotic etal. PRC71, 044319(2005).

ALL ARE EQUIVALENTS.

Weak–nuclear interaction

Reaction:

$$\nu_l + (Z, A) \rightarrow (Z+1, A) + l^-$$

Weak hamiltonian:

$$H_W(\vec{r}) = \frac{G}{\sqrt{2}} J_\alpha l_\alpha e^{-i\vec{k}\cdot\vec{r}}$$

$$J_\alpha = i\gamma_4\left[g_V\gamma_\alpha - \frac{g_M}{2\mathrm{M}}\sigma_{\alpha\beta}k_\beta + g_A\gamma_\alpha\gamma_5 + i\frac{g_P}{\mathrm{m}_\ell}k_\alpha\gamma_5\right] \qquad l_\alpha = -i\bar{u}_{s_\ell}(\mathbf{p}, E_\ell)\gamma_\alpha(1+\gamma_5)u_{s_\nu}(\mathbf{q}, E_\nu)$$

Neutrino-nucleus cross section (Fermi's Golden Rule):

$$\sigma(E_l, J_f) = \frac{p_l E_l}{2\pi} F(Z+1, E_l)\int_{-1}^{1} d(\cos\theta) T_\sigma(|\vec{k}|, J_f)$$

p_l :Lepton momentum, E_l : Lepton energy, *F(Z+1,E):* Fermi function

Transition amplitude

$$\mathrm{T}_\sigma(|\vec{k}|, J_f) \equiv \frac{1}{2J_i+1}\sum_{s_l s_\nu}\sum_{M_f M_i}|\langle J_f M_f \,|\, H_W \,|\, J_i M_i\rangle|^2 = \frac{G^2}{2J_i+1}\sum_{M_f M_i}\mathrm{O}_\alpha \mathrm{O}^*_\beta L_{\alpha\beta}$$

$\mathrm{O}_\alpha = \langle J_f \,||\, J_\alpha e^{-i\vec{k}\cdot\vec{r}} \,||\, J_i\rangle,$ Nuclear Matrix Element , Lepton traces $L_{\alpha\beta}$

$k = (\vec{k}, k_\varnothing), \rho = \kappa.r = |\vec{k}|.r$ Transfer momentum, with **k**= **|k|** ž.

$$J_\emptyset = g_\mathrm{V} + (\bar{g}_\mathrm{A} + \bar{g}_{\mathrm{P}1})\boldsymbol{\sigma}\cdot\hat{\mathbf{k}} + ig_A\mathrm{M}^{-1}\boldsymbol{\sigma}\cdot\boldsymbol{\nabla},$$

Hadronic current (non-relativistic)

$$\mathbf{J} = -g_\mathrm{A}\boldsymbol{\sigma} - i\bar{g}_\mathrm{W}\boldsymbol{\sigma}\times\hat{\mathbf{k}} - \bar{g}_\mathrm{V}\hat{\mathbf{k}} + \bar{g}_{\mathrm{P}2}(\boldsymbol{\sigma}\cdot\hat{\mathbf{k}})\hat{\mathbf{k}} - ig_V\mathrm{M}^{-1}\boldsymbol{\nabla},$$

Weak–nuclear interaction

Non-relativistic approximation of hadronic current

$$J_\emptyset = g_V + (\overline{g}_A + \overline{g}_{P1})\boldsymbol{\sigma}\cdot\hat{\mathbf{k}} + i g_A M^{-1}\boldsymbol{\sigma}\cdot\boldsymbol{\nabla},$$

$$\mathbf{J} = -g_A\boldsymbol{\sigma} - i\overline{g}_W\boldsymbol{\sigma}\times\hat{\mathbf{k}} - \overline{g}_V\hat{\mathbf{k}} + \overline{g}_{P2}(\boldsymbol{\sigma}\cdot\hat{\mathbf{k}})\hat{\mathbf{k}} - i g_V M^{-1}\boldsymbol{\nabla},$$

Nuclear coupling constant

$$g_V = 1, \quad g_A = 1.26,$$

$$g_M = \kappa_p - \kappa_n = 3.70, \quad g_P = g_A\frac{2Mm_\ell}{k^2 + m_\pi^2}.$$

FNS effect: $g \rightarrow g\left(\frac{\Lambda^2}{\Lambda^2 + k^2}\right)^2$

Λ=850 MeV

Transfer momentum, with **k**= |**k**| ž.

$$e^{-i\mathbf{k}\cdot\mathbf{r}} = \sum_L i^{-L}\sqrt{4\pi(2L+1)}\,j_L(\kappa r)Y_{L0}(\hat{\mathbf{r}}),$$

Elementary Operators :

$$\mathcal{M}_J^V = j_J(\rho)Y_J(\hat{\mathbf{r}}),$$

$$\mathcal{M}_J^A = \kappa^{-1}j_J(\rho)Y_J(\hat{\mathbf{r}})(\boldsymbol{\sigma}\cdot\boldsymbol{\nabla}),$$

$$\mathcal{M}_{MJ}^A = \sum_L i^{J-L-1}\,F_{MLJ}j_L(\rho)\,[Y_L(\hat{\mathbf{r}})\otimes\boldsymbol{\sigma}]_J\,,$$

$$\mathcal{M}_{MJ}^V = \kappa^{-1}\sum_L i^{J-L-1}F_{MLJ}j_L(\rho)[Y_L(\hat{\mathbf{r}})\otimes\boldsymbol{\nabla}]_J$$

Weak–nuclear interaction

$$\mathcal{T}_\sigma(\kappa, J_f) = \frac{4\pi G^2}{2J_i+1}\sum_{\mathsf{J}}\left[|\langle J_f||\mathsf{O}_{\emptyset\mathsf{J}}||J_i\rangle|^2\mathcal{L}_\emptyset + \sum_{\mathsf{M}=0,\pm1}|\langle J_f||\mathsf{O}_{\mathsf{MJ}}||J_i\rangle|^2\mathcal{L}_{\mathsf{M}}\right.$$
$$\left. - 2\Re(|\langle J_f||\mathsf{O}_{\emptyset\mathsf{J}}||J_i\rangle\langle J_f||\mathsf{O}_{0\mathsf{J}}||J_i\rangle)\mathcal{L}_{\emptyset 0}\right].$$

$L_{;}$ L_M $L_{;0}$ Lepton Traces

☺ For natural parity states with $\pi=(-)^J$,i.e., 0^+, 1^- , 2^+, 3^-….

$$\mathsf{O}_{\emptyset\mathsf{J}} = g_V\mathcal{M}^V_{\mathsf{J}}$$
$$\mathsf{O}^{CVC}_{0\mathsf{J}} = \frac{k_\emptyset}{\kappa}g_V\mathcal{M}^V_{\mathsf{J}}$$
$$\mathsf{O}_{0\mathsf{J}} = 2\overline{g}_V\mathcal{M}^V_{0\mathsf{J}} - \overline{g}_V\mathcal{M}^V_{\mathsf{J}}$$
$$\mathsf{O}_{\mathsf{M}\neq0\mathsf{J}} = (\mathsf{M}g_A - \overline{g}_W)\hat{\mathcal{M}}^A_{1\mathsf{J}} + 2\overline{g}_V\tilde{\mathcal{M}}^V_{1\mathsf{J}}$$

☺ For unnatural parity states with $\pi=(-)^{J+1}$,i.e., 0^-, 1^+ ,2^-, 3^+….

$$-i\mathsf{O}_{\emptyset\mathsf{J}} = 2\overline{g}_A\mathcal{M}^A_{\mathsf{J}} + (\overline{g}_A + \overline{g}_{P1})\mathcal{M}^A_{0\mathsf{J}}$$
$$-i\mathsf{O}_{0\mathsf{J}} = (\overline{g}_{P2} - g_A)\mathcal{M}^A_{0\mathsf{J}}$$
$$-i\mathsf{O}_{\mathsf{M}\neq0\mathsf{J}} = (-g_A + \mathsf{M}\overline{g}_W)\tilde{\mathcal{M}}^A_{1\mathsf{J}} + 2\mathsf{M}\overline{g}_V\hat{\mathcal{M}}^V_{1\mathsf{J}}$$

(i) deForest Jr.& Walecka, Adv.Phys15, 1(1966)
(ii) Kuramoto etal. NPA 512, 711 (1990)
(iii) Luyten etal. NP41,236 (1963)(μ-capture)
(iv) Krmpotic etal. PRC71, 044319(2005).

≈ all are equivalents.

$$\mathsf{O}_{\emptyset\mathsf{J}} = \hat{\mathcal{M}}_{\mathsf{J}},$$
$$\mathsf{O}_{\mathsf{MJ}} = \begin{cases} \hat{\mathcal{L}}_{\mathsf{J}}, & \text{for} \quad \mathsf{M}=0 \\ -\frac{1}{\sqrt{2}}\left[\mathsf{M}\hat{T}^{MAG}_{\mathsf{J}} + \hat{T}^{EL}_{\mathsf{J}}\right], & \text{for} \quad \mathsf{M}=\pm1 \end{cases}$$

Nuclear Structure Models

(i) Models with **microscopical formalism** with detailed nuclear structure, solves the microscopic quantum-mechanical Schrodinger or Dirac equation, provides nuclear wave functions and (g.s.-shape E_{sp} , J^{π} , log (ft), $\tau_{1/2}$ …)

Examples:

Shell Model (Martinez et al. PRL83, 4502(1999))

RPA models

Self-Consistent Skyrme-HFB+QRPA

(Engel etal. PRC60, 014302(1999))

QRPA, Projected QRPA

(Krmpotic etal. PLB319(1993)393.)

Relativistic QRPA

(N. Paar et al., Phys. Rev. C 69, 054303 (2004))

Density Functional+Finite Fermi Syst.

(Borzov etal. PRC62, 035501 (2000))

(ii) Models describing **overall nucler properties** statistically where the parameters are adjusted to exp. data, no nuclear wave funct., polynomial or algebraic express.

Examples:

Fermi Gas Model,

Gross Theory of β-decay (GTBD)

Takahashi etal. PTP41,1470 (1969)

New exponential law for β^{+}.....

(Zhang etal. PRC73,014304(2006))

$\tau_{1/2}$ (Kar etal., astro-ph/06034517(2006))

Nuclear Structure Models

SHELL MODEL → accurate in description of the ground state wave functions, description of high-lying states necessitates a large model space which is problematic to treat numerically

Different interactions in various mass regions employed, only lower mass nuclei can be studied

The interacting shell model is **the** method of choice for weak interactions (β-decay, ν-capture, e^--capture) **Why?**

Pauli blocking/ unblocking

example:

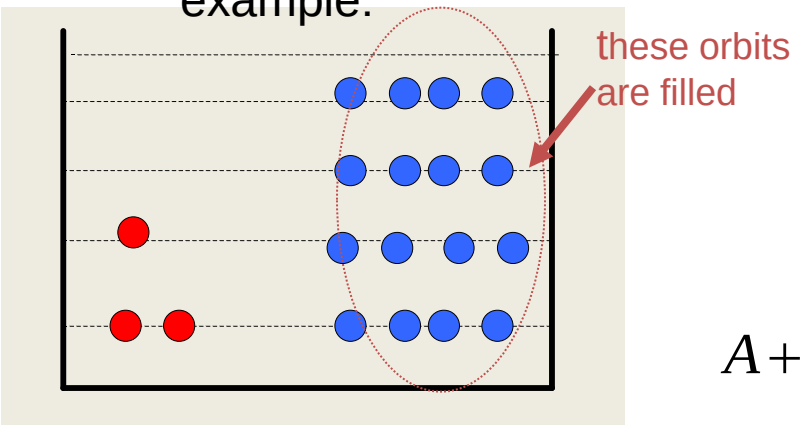

"Hartree-Fock configuration"

Now consider neutrino and anti-neutrino capture

$$A + \nu_e \rightarrow B + e^-$$

OK!

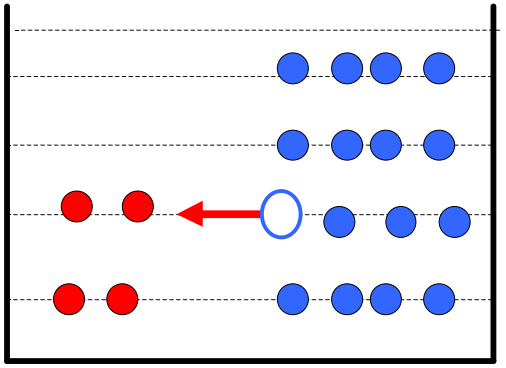

HYPERSIMPLE SCHEME

Nuclear Structure Models

$$A + \bar{\nu}_e \rightarrow C + e^+$$

NO!
Pauli blocked!

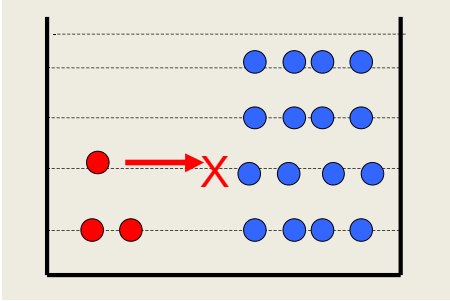

NO! requires too much energy!!

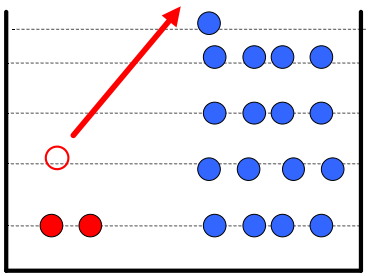

But, if $\Psi =$

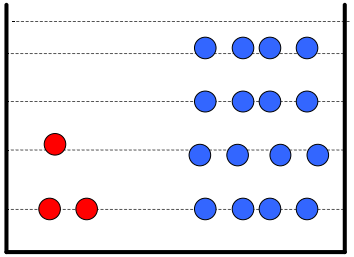

$+$

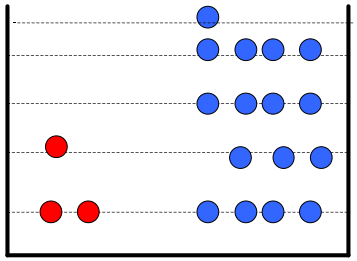

$+ \ldots$

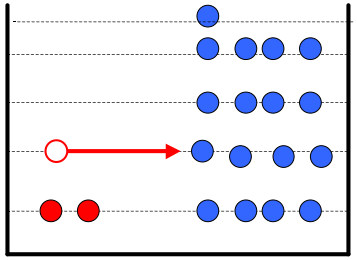

OK!

HYPERSIMPLE SCHEME

Some weak processes (usually $p \rightarrow n$) blocked because neutron orbits already occupied. But configuration mixing, even a little, can **unblock** by creating holes for the new neutron to go into.
thus: **Weak processes sensitive to configuration mixing**

For example: "... the total GT strength for 56Fe in the complete pf shell involving 7 413 488 J=0+ configurations (this corresponds to an m-scheme dimension of 501 million).
E. Kolbe et al., PHYSICAL REVIEW C, VOLUME 60, 052801

Nuclear Structure Models

QRPA: Quasiparticle Random Phase Approximation

$$(e_t - \lambda_t)(u_t^2 - v_t^2) + u_t v_t \Delta_t = 0,$$

$$\begin{pmatrix} \mathcal{A} & \mathcal{B} \\ \mathcal{B} & \mathcal{A} \end{pmatrix} \begin{pmatrix} X \\ Y \end{pmatrix} = \omega \begin{pmatrix} X \\ -Y \end{pmatrix},$$

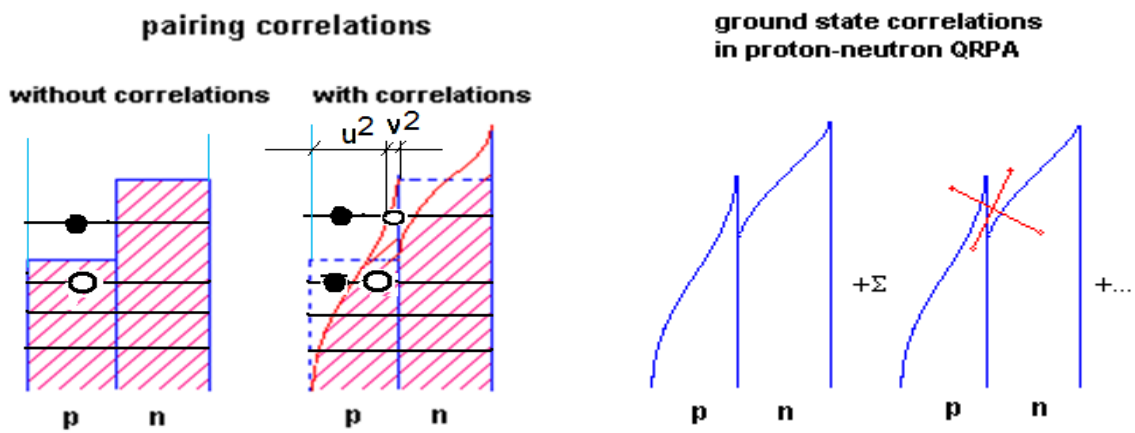

$$\langle BCS|\hat{N}|BCS\rangle \equiv \sum_{t=n(p)} (2j_t + 1) v_{jt}^2 = N(Z),$$

PQRPA: Projected QRPA

$$2\hat{e}_p u_p v_p - \Delta_p (u_p^2 - v_p^2) \;=\; 0,$$

Particle number is conserved exactly .

Krmpotic etal. PLB319(1993)393.

$$\begin{pmatrix} \mathcal{A}_\mu & \mathcal{B} \\ -\mathcal{B}^\dagger & -\mathcal{A}^*_{-\mu} \end{pmatrix} \begin{pmatrix} \mathcal{X}_\mu \\ \mathcal{Y}_\mu \end{pmatrix} = \Omega_\mu \begin{pmatrix} \mathcal{X}_\mu \\ \mathcal{Y}_\mu \end{pmatrix},$$

$$V = -4\pi \left(v_s P_s + v_t P_t\right) \delta(r),$$

Nuclear Structure Models

RQRPA: Relativistic Quasiparticle Random Phase *

$$(e_t - \lambda_t)(u_t^2 - v_t^2) + u_t v_t \Delta_t = 0,$$

$$\begin{pmatrix} \mathcal{A} & \mathcal{B} \\ \mathcal{B} & \mathcal{A} \end{pmatrix} \begin{pmatrix} X \\ Y \end{pmatrix} = \omega \begin{pmatrix} X \\ -Y \end{pmatrix},$$

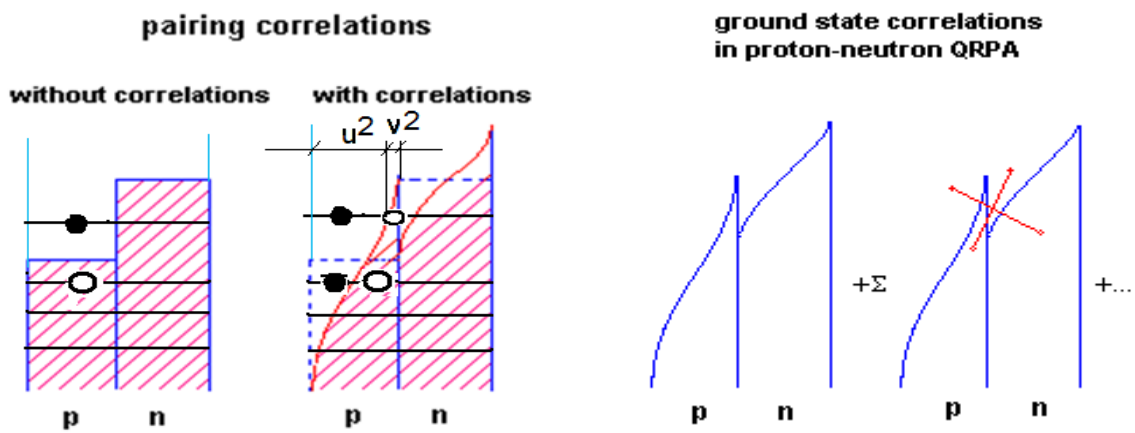

- RQRPA where both the mean field and the residual interaction are derived from the same effective Lagrangian density [9]. The ground state is calculated in the Relativistic Hartree-Bogoliubov (RHB) model using effective Lagrangians with density dependent meson-nucleon couplings and DD-ME2 parameterization, and pairing correlations are described by the finite range Gogny force. The HO basis with $N = 20$ or $N = 30$ is used only in the RHB calculation in order to determine the ground state and the single-particle spectra. The wave functions employed in RPA equations are obtained by converting the original basis to the coordinate representation, and the size of the RQRPA configuration space is limited by $2qp$ energy cut-offs E_{2qp}.

* N. Paar et al., Phys. Rev. C 69, 054303 (2004)

QRPA/PQRPA in ^{12}C

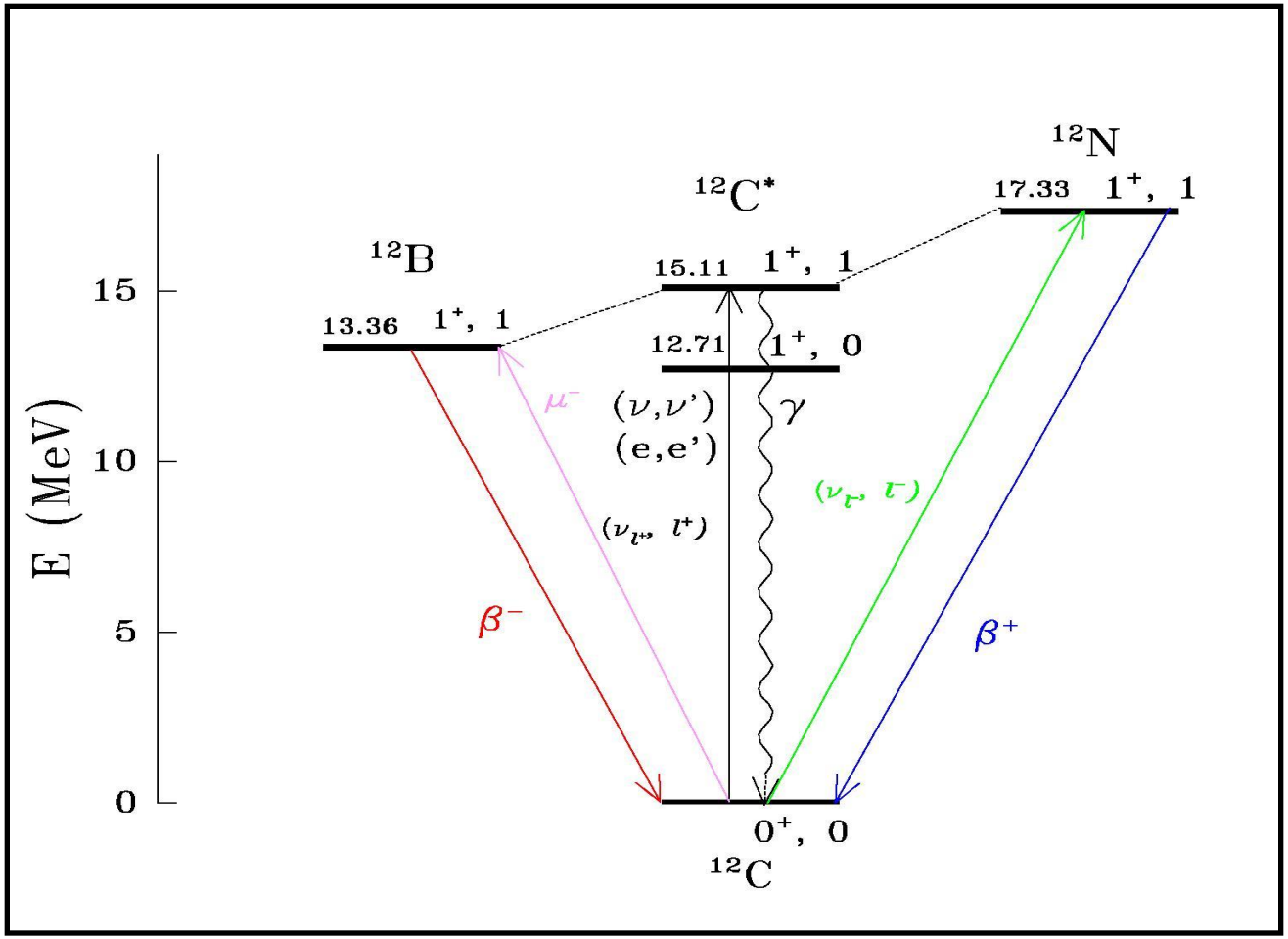

- Neutrino Scattering (NS)

$$\nu_l + (Z, A) \rightarrow (Z+1, A) + l^-$$

- Anti - neutrino Scattering (AS)

$$\bar{\nu}_l + (Z, A) \rightarrow (Z-1, A) + l^+$$

- Muon Capture (MC) rate

$$\mu^- + (Z, A) \rightarrow (Z-1, A) + \nu_\mu$$

- Beta decay

$$(Z \pm 1, A) \rightarrow (Z, A) + e^\pm + \nu_e(\bar{\nu}_e)$$

$$\langle J_f, Z+\mu, N-\mu \| \mathrm{Y}_J \| 0^+ \rangle = \frac{1}{(I^Z I^N)^{1/2}} \sum_{pn} \left[\frac{\Lambda_\mu(pnJ)}{(I^{Z-1+\mu}(p) I^{N-1+\mu}(n))^{1/2}} X^*_\mu(pnJ_f) + \frac{\Lambda_{-\mu}(pnJ)}{(I^{Z-1-\mu}(p) I^{N-1-\mu}(n))^{1/2}} Y^*_\mu(pnJ_f) \right], \qquad (3.1)$$

$$\Lambda_\mu(pnJ) = -\frac{\langle p \| \mathrm{Y}_J \| n \rangle}{\sqrt{2J+1}} \begin{cases} u_p v_n, & \text{for } \mu = +1, \\ u_n v_p, & \text{for } \mu = -1, \end{cases}$$

QRPA/PQRPA in ^{12}C

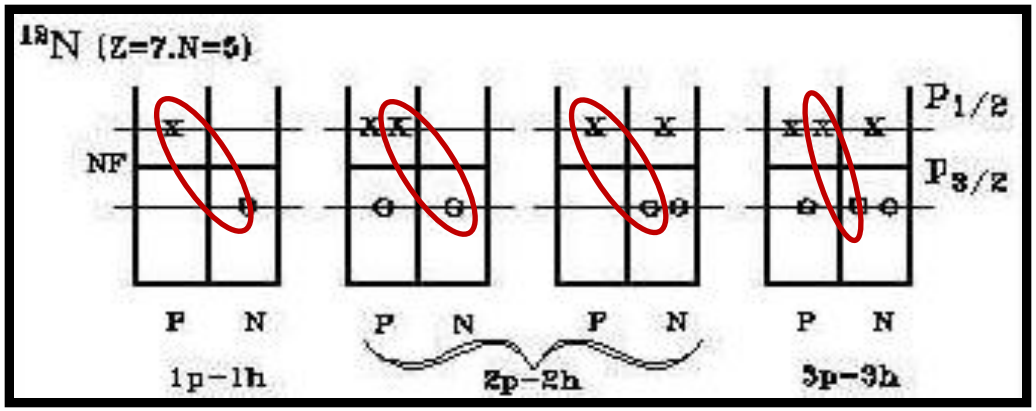

Volpe etal , PRC 62 (2000)

``difficulties in choosing the g.s. of 12N because the lowest state is not the most collective one"

$$V = -4\pi\,(v_s P_s + v_t P_t)\,\delta(r),$$

ph-channel parameters from systematic study GT resonances, F.K.&S.S. NPA 572, 329(1994)

P (I) : $v_s^{ph} = v^{pair}$, $v_t^{ph} = v_s^{ph}/0.6$

P(II): $v_s^{ph} = 27$, $v_t^{ph} = 64$

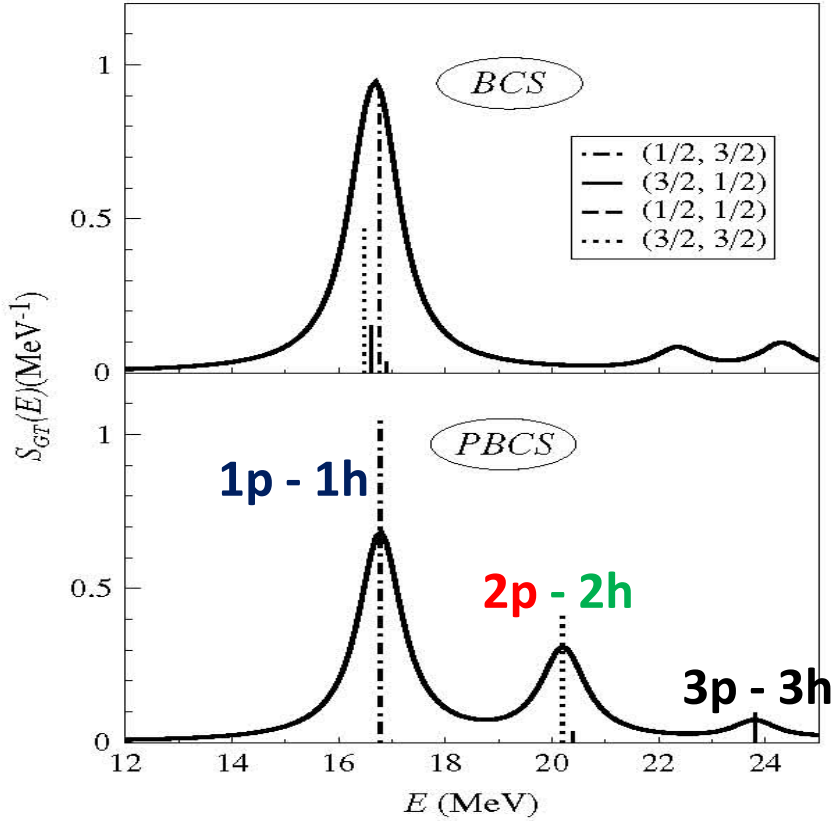

$$(v_s^{PP} \equiv v_s^{pair} \text{ and } v_t^{PP} \gtrsim v_s^{PP})$$

$$t = \frac{2v_t^{PP}}{v_s^{pair}(p) + v_s^{pair}(n)},$$

QRPA/PQRPA in ^{12}C

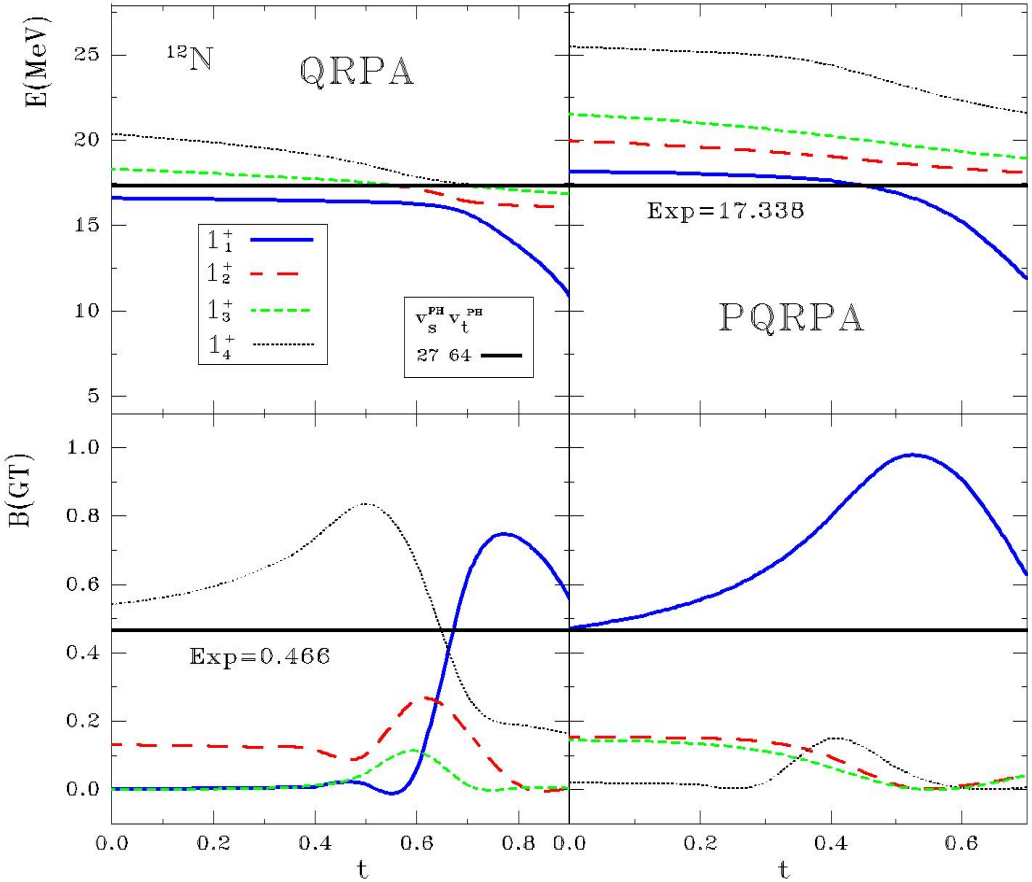

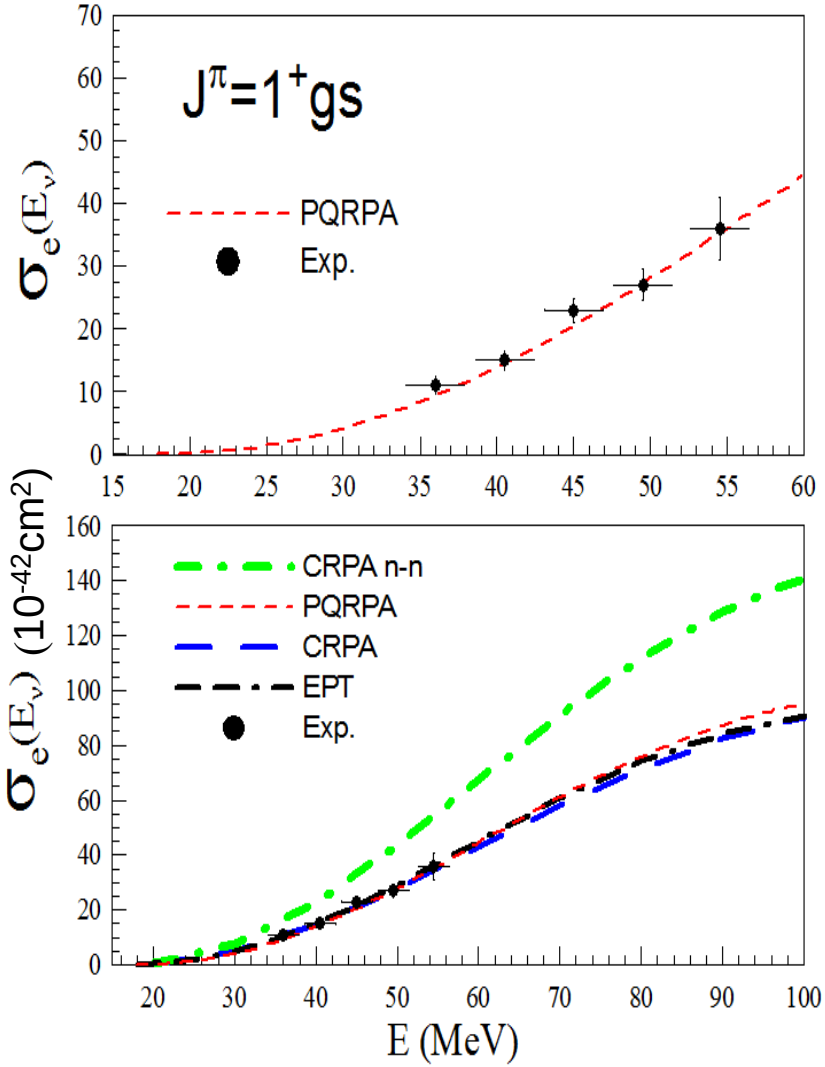

Projection Procedure is Important!

Krmpotic etal. PRC71, 044319(2005).

CRPA, Kolbe etal., PRC71, 044319(2005).
EPT, Mintz, PRC25,1671(1982).
PQRPA, Krmpotic etal., PRC71, 044319 (2005).
Exp, LSND coll., PRC55, 2078(1997).

QRPA/PQRPA in ^{12}C

TABLE V. Experimental and calculated muon-capture rate in units of 10^3 s^{-1}. The full PQRPA calculations, which include the relativistic corrections, are listed for all three parametrizations. Theoretical results that involve only the velocity-independent matrix elements are displayed in parentheses in the third column for the case PII. The rates are grouped by their degrees of forbiddeness. We show (i) the exclusive rates $\Lambda(J^\pi)$, for $J_f^\pi = 1_1^+, 1_1^-, 2_1^-, 2_1^+$, (ii) the multipole decomposition of the rates $\sum_f \Lambda(J_f^\pi)$ for each final state with spin and parity J_f^π, and (iii) the inclusive decay rate $\Lambda^{\rm inc} \equiv \sum_{J_f^\pi} \Lambda(J_f^\pi)$. In the fourth column are listed the results of recent SM calculations, which are explained in the text. The measured capture rates are given in the last column.

Muon-capture rate	PQRPA			Shell model			Experiment
	(I)	(II)	(III)	SM1 [16]	SM2 [16]	SM3 [17]	
Allowed		49.3%		39.3%			
$\Lambda(1_1^+)$	7.52	6.27(6.50)	6.27	11.56	6.3	6.0	6.2 ± 0.3 [33]
$\sum_f \Lambda(0_f^+)$	3.68	2.86(3.15)	3.77	0.21			
$\sum_f \Lambda(1_f^+)$	20.28	18.14(18.63)	18.22	15.43			
First forbidden		46.6%		55.7%			
$\Lambda(1_1^-)$	1.06	0.49(0.51)	0.98			1.86	0.62 ± 0.20 [34,35]
$\Lambda(2_1^-)$	0.31	0.18(0.18)	0.16			0.22	0.18 ± 0.10 [34,35]
$\sum_f \Lambda(0_f^-)$	2.62	2.35(0.72)	2.35	2.12			
$\sum_f \Lambda(1_f^-)$	11.84	10.37(9.51)	11.37	12.25			
$\sum_f \Lambda(2_f^-)$	7.78	7.12(6.90)	7.15	7.79			
Second forbidden		3.9%		4.6%			
$\Lambda(2_1^+)$	0.19	0.14(0.16)	0.15			0.25	0.21 ± 0.10 [34,35]
$\sum_f \Lambda(2_f^+)$	1.26	1.09(0.89)	1.17	1.36			
$\sum_f \Lambda(3_f^+)$	0.63	0.57(0.57)	0.58	0.46			
$\Lambda^{\rm inc}$	48.16	42.56(40.7)	44.67	39.82	41.9	33.5	38 ± 1 [36]

QRPA/PQRPA in ^{12}C

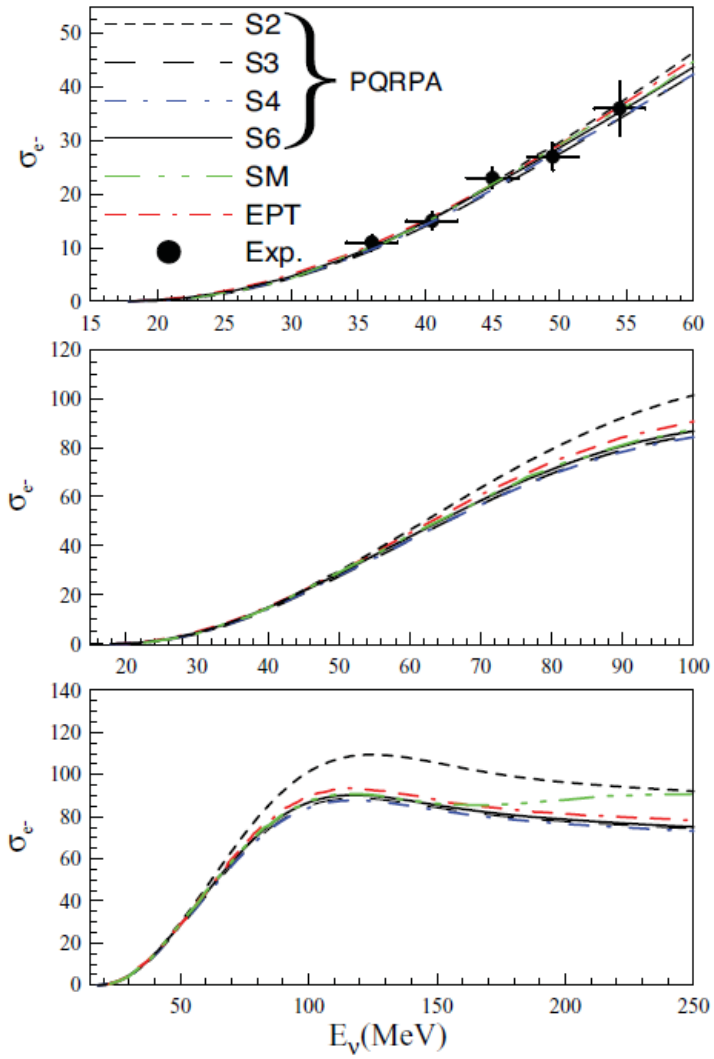

FIG. 3. (Color online) Same as Fig. 2, but here $t = 0$ for S_2 and S_3, $t = 0.2$ for S_4, and $t = 0.3$ for S_6. SM and EPT calculations are, respectively, from Refs. [98] and [16]. Experimental data in the DAR region are from Ref. [25].

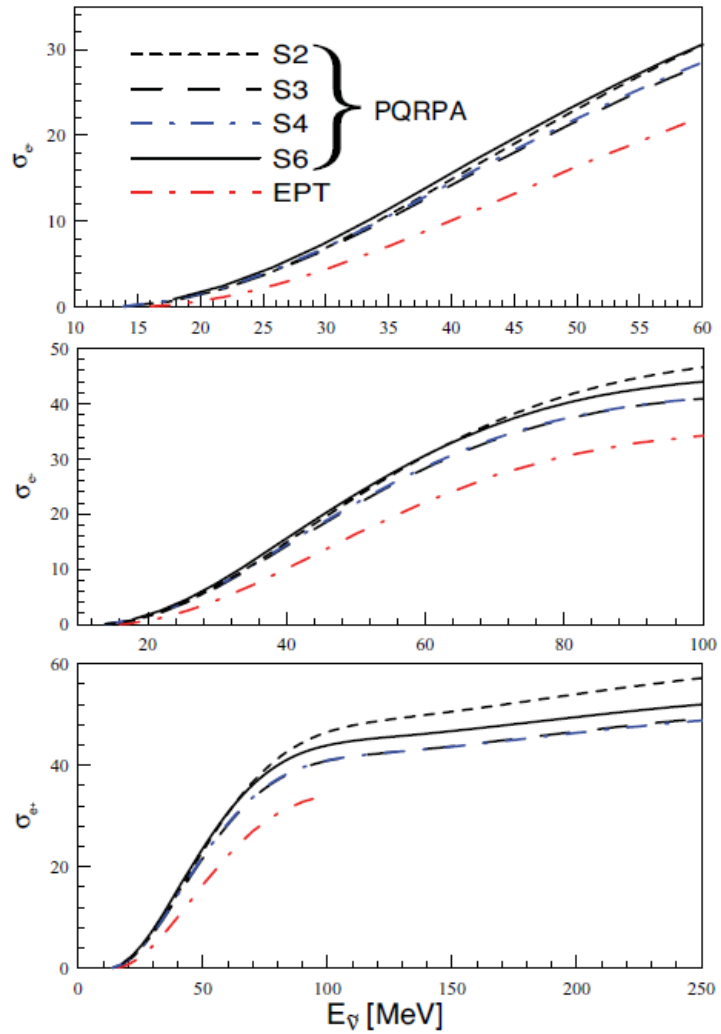

FIG. 4. (Color online) Calculated $^{12}C(\bar\nu, e^+)^{12}B$ cross section $\sigma_{e^+}(E_{\bar\nu}, 1_1^+)$ (in units of 10^{-42} cm^2), plotted as a function of the incident antineutrino energy $E_{\bar\nu}$. As in Fig. 3, the value of t is 0 for s.p. spaces S_2, and S_3, 0.2 for S_4, and 0.3 for S_6. The EPT calculation from Ref. [16] is also shown.

QRPA/PQRPA/RQRPA in ^{12}C

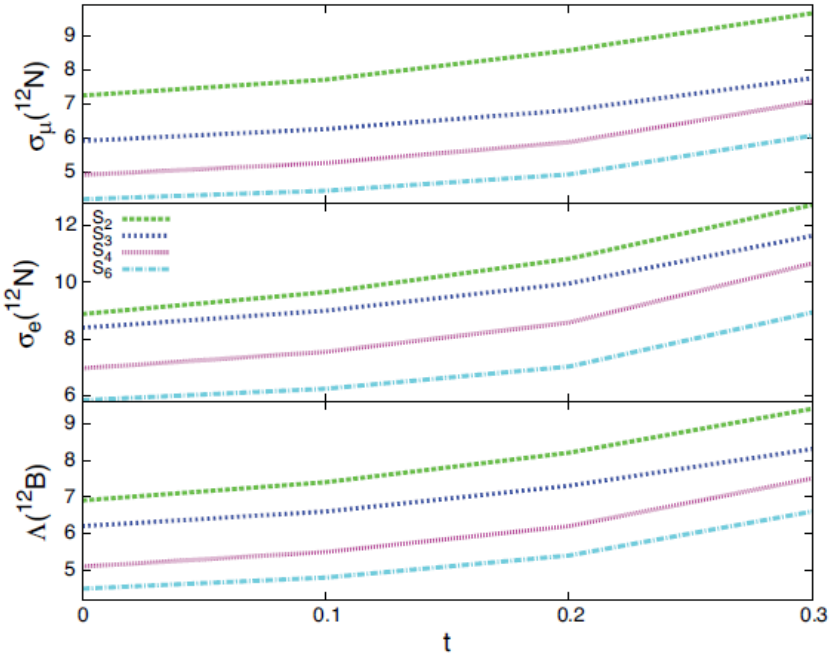

FIG. 5. (Color online) Muon-capture transition rate to the ^{12}B ground state (in units of 10^2 s^{-1}, and electron and muon folded ECSs to the ^{12}N ground state in units of 10^{-42} cm^2 and 10^{-41} cm^2, respectively. Experimental values, in these units, are $\Lambda(^{12}\mathrm{B}) = 6.2 \pm 0.3$ [45], $\overline{\sigma}_e(^{12}\mathrm{N}) = 9.1 \pm 0.4 \pm 0.9$ [25], and $\overline{\sigma}_e(^{12}\mathrm{N}) = 8.9 \pm 0.3 \pm 0.9$ [26] and $\overline{\sigma}_\mu(^{12}\mathrm{N}) = 6.6 \pm 1.0 \pm 1.0$ [28], and $\overline{\sigma}_\mu(^{12}\mathrm{N}) = 5.6 \pm 0.8 \pm 1.0$ [29], respectively.

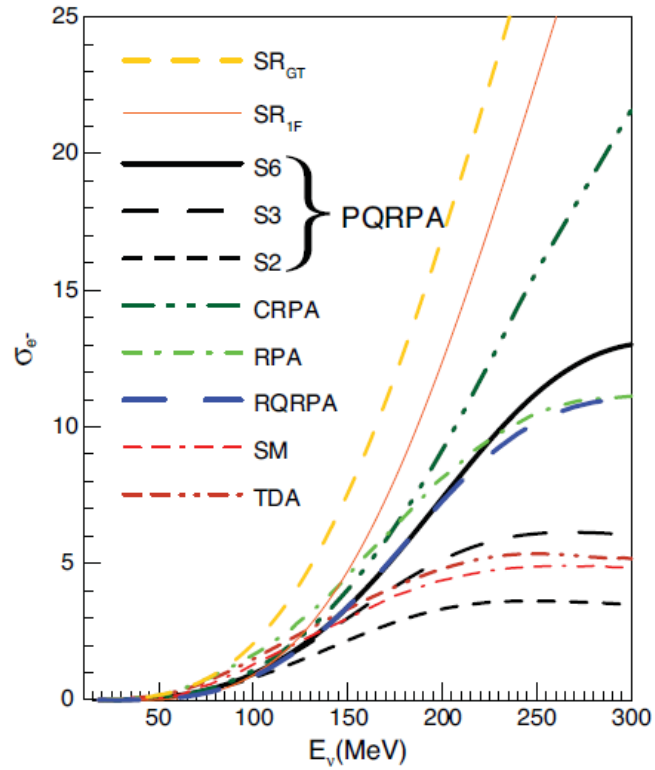

FIG. 6. (Color online) Inclusive $^{12}\mathrm{C}(\nu, e^-)^{12}\mathrm{N}$ cross section $\sigma_{e^-}(E_\nu)$ (in units of 10^{-39} cm^2) plotted as a function of the incident neutrino energy E_ν. PQRPA results within s.p. spaces S_2, S_3, and S_6, and with the same values of $s = t$ as in Fig. 3, are compared with two sum-rule limits (as explained in the text), $\mathrm{SR_{GT}}$ and $\mathrm{SR_{1F}}$, obtained with an average excitation energy $\overline{\omega_{J_n^\pi}}$ of 17.34 and 42 MeV, respectively. Several previous RPA-like calculations, namely, the RPA [43], CRPA [102], and RQRPA within S_{20} for $E_{2qp} = 100$ MeV [51], as well as the SM [43] and the TDA [34], are also shown.

CRPA/PQRPA in ^{12}C

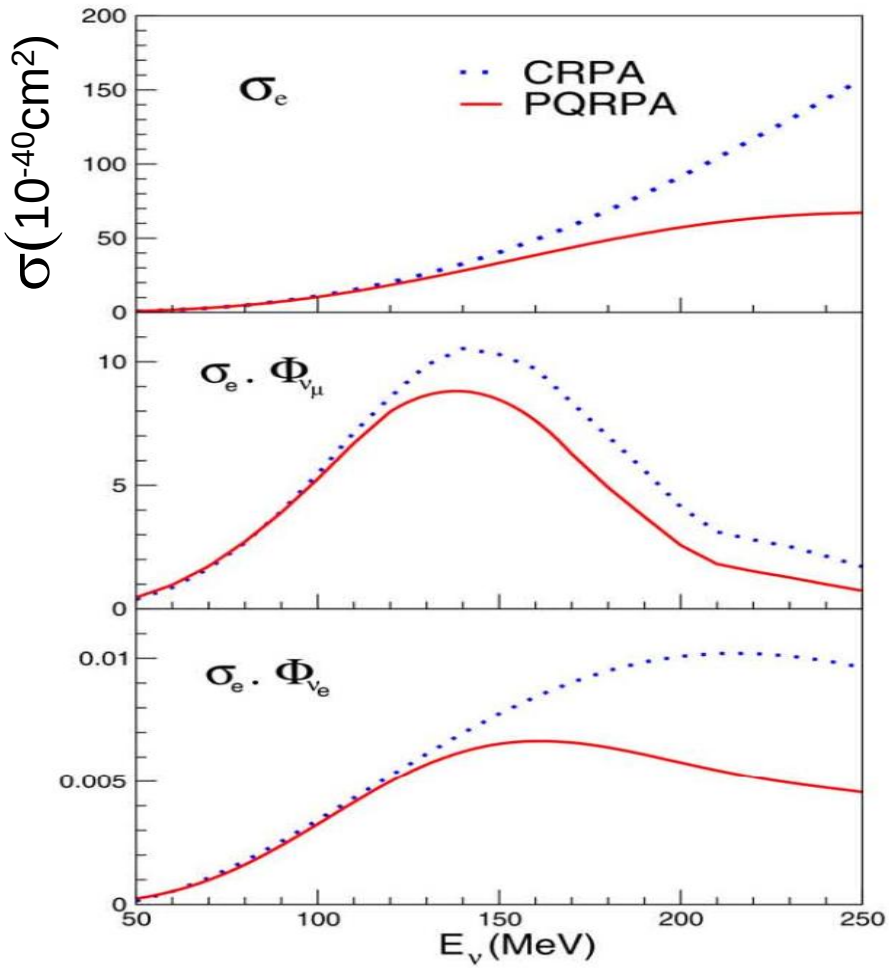

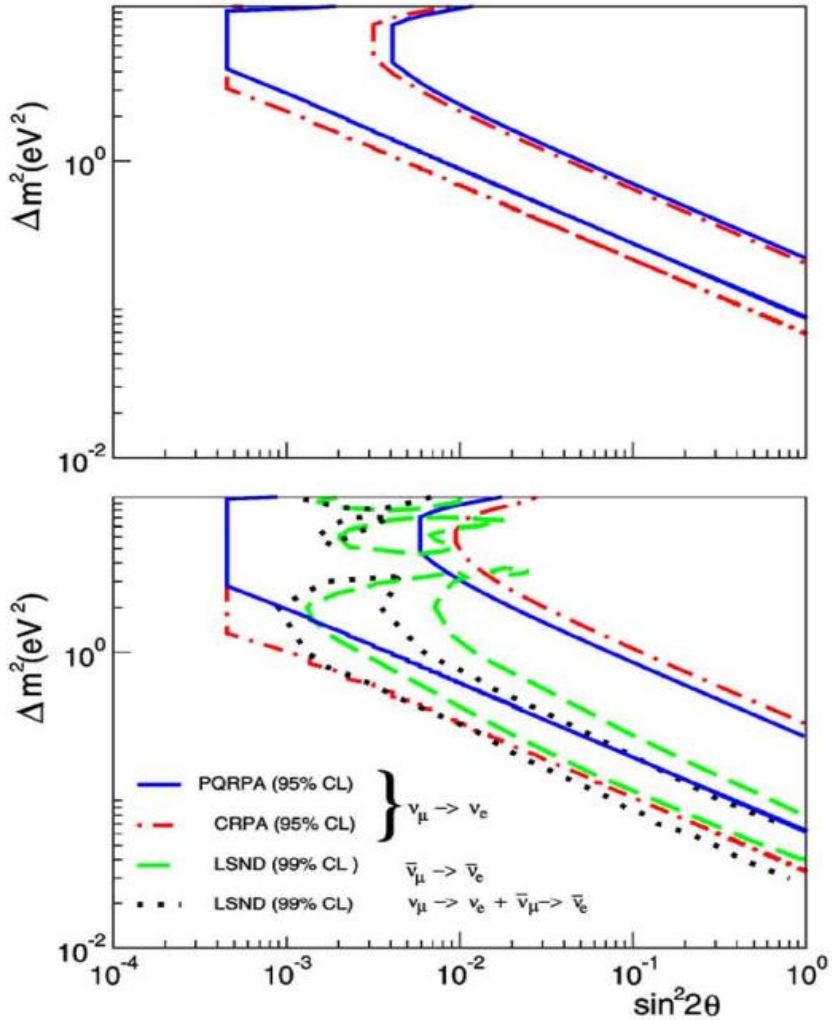

ν-nucleus cross section are important to constrain parameters in neutrino oscillations.

$$\bar{\nu}_\mu \rightarrow \bar{\nu}_e \qquad \nu_\mu \rightarrow \nu_e$$

* Increase probability oscillations.
* Confidence level region is diminished by difference in σ_e between PQRPA and CRPA,

A.Samana,F. Krmpotic,A. Marianoc,R. Zukanovich Funchal PLB (2005) 100

QRPA/PQRPA/RQRPA in ^{12}C

TABLE I. Fraction (in %) of flux-averaged cross sections $\overline{\sigma}_{e^+}$ for $^{12}C(\tilde{\nu}, e^+)^{12}B$ for allowed (A), first forbidden (1F), second forbidden (2F), and third forbidden (3F) processes. Antineutrino fluxes $n_{e^+}(E_{\tilde{\nu}})$ are the same as in Ref. [108], that is, the DAR flux, and those produced by boosted ^{6}He ions with different values of $\gamma = 1/\sqrt{1 - v^2/c^2}$. Results of two calculations are presented: (i) PQRPA within S_5 and (ii) RQRPA within $N = 30$, with a cutoff $E_{2qp} = 300$ MeV.

	DAR	γ		
		6	10	14
A				
PQRPA	79.43	92.09	77.00	63.01
RQRPA	84.40	94.88	82.25	67.15
1F				
PQRPA	20.03	7.83	22.16	33.76
RQRPA	15.10	4.13	16.86	29.61
2F				
PQRPA	0.51	0.07	0.78	2.89
RQRPA	0.55	0.08	0.81	2.91
3F				
PQRPA	0.018	0.002	0.04	0.33
RQRPA	0.025	0.011	0.05	0.33

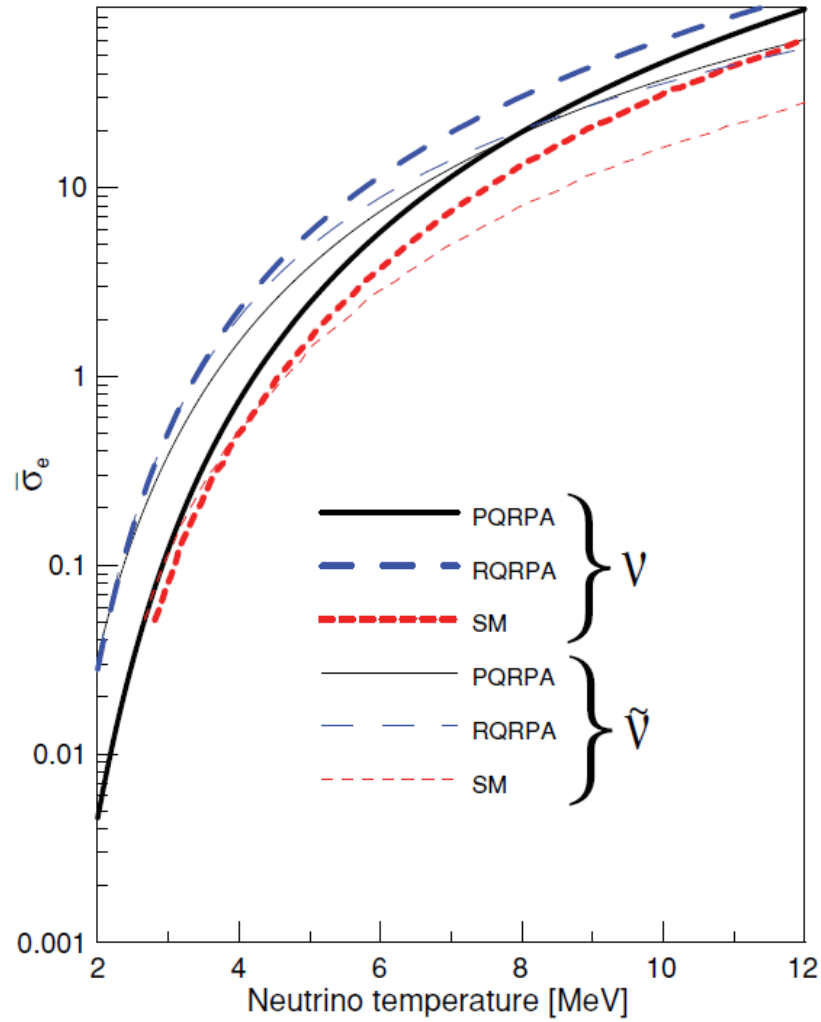

FIG. 13. (Color online) Flux-averaged neutrino and antineutrino cross sections $\overline{\sigma}_{e^\pm}$ in ^{12}C with typical supernova fluxes.

RQRPA in ^{12}C

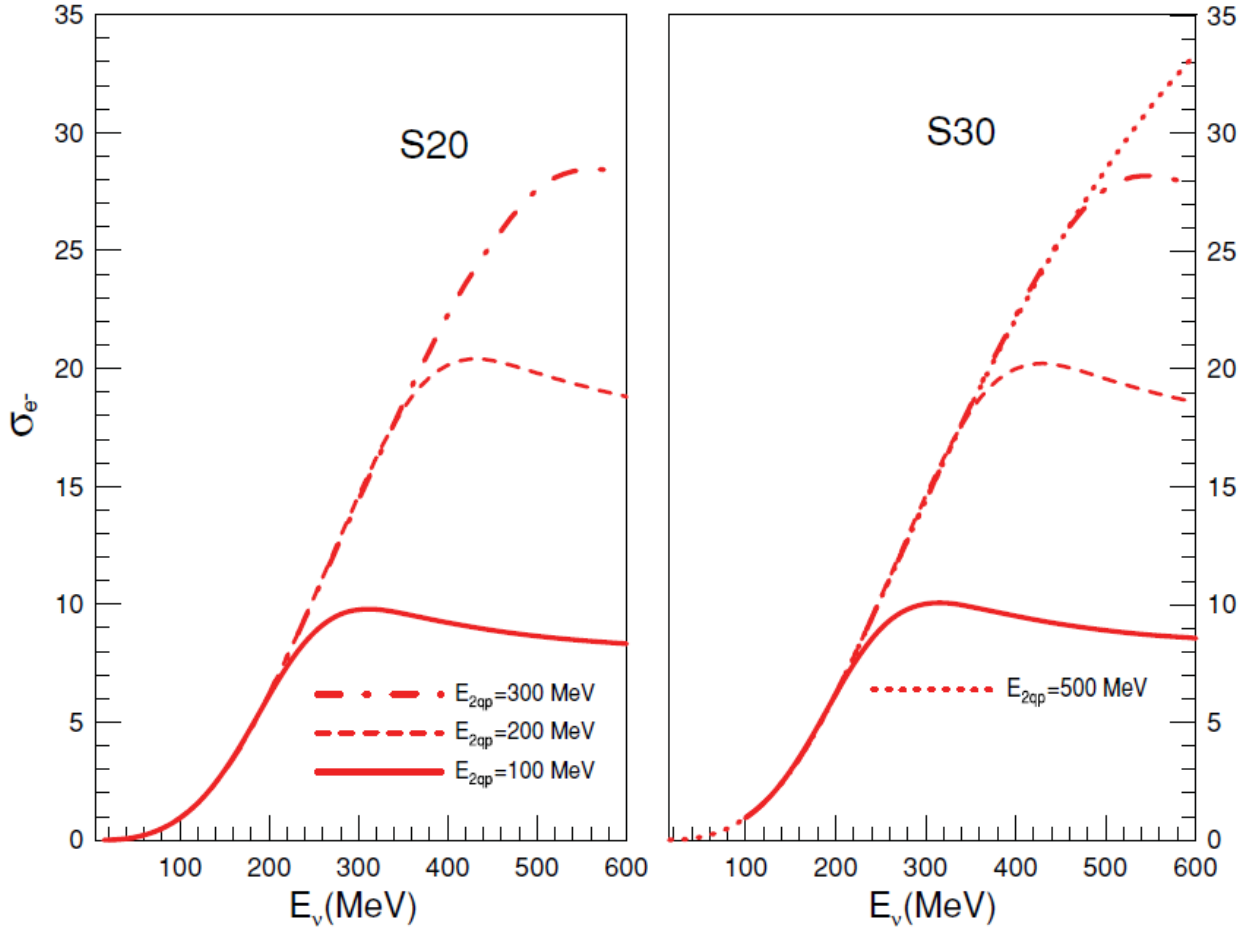

FIG. 8. (Color online) Inclusive $^{12}C(\nu, e^-)^{12}N$ cross-section $\sigma_{e^-}(E_\nu)$(in units of 10^{-39} cm^2) plotted as a function of the incident neutrino energy E_ν, evaluated in RQRPA with different configuration spaces. These cross sections are plotted as functions of the incident neutrino energy with different cut-off of the E_{2qp} quasiparticle energy as it is explained in the text. The left and right panels show the cross section evaluated with S_{20}, and S_{30} s.p. spaces. The last cross section shows that the convergence of the calculation is achieved up to 600 MeV of incident neutrino energy.

RQRPA in ^{12}C

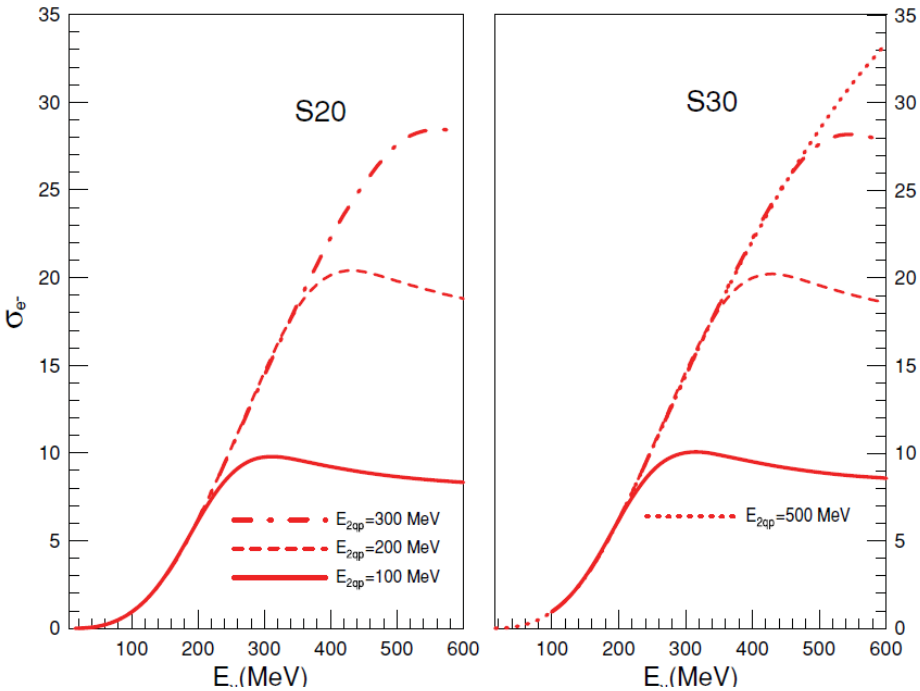

Inclusive $^{12}C(\nu, e-)^{12}N$ cross-section σ_{e-} ($E\nu$)(in units of 10−39 cm2) plotted as a function of the incident neutrino energy $E\nu$, evaluated in RQRPA with different configuration spaces. These cross sections are plotted as functions of the incident neutrino energy with different cut-off of the E_{2qp} quasiparticle energy as it is explained in the text. The left and right panels show the cross section evaluated with *S*20, and *S*30 s.p. spaces. The last cross section shows that the convergence of the calculation is achieved up to 600 MeV of incident neutrino energy.

Left and right panels show, respectively, the cross sections $\sigma_{e-}(E\nu)$, and σ_{e+} ($E\tilde{\nu}$) (in units of 10^{-39} cm^2) evaluated in RQRPA for *S*20, and *S*30 s.p. spaces with the cutoff E_{2qp} = 500 MeV, and different maximal values of J±, with J going from 1 up to 14 for neutrinos, and from 1 up to 11 for antineutrinos.

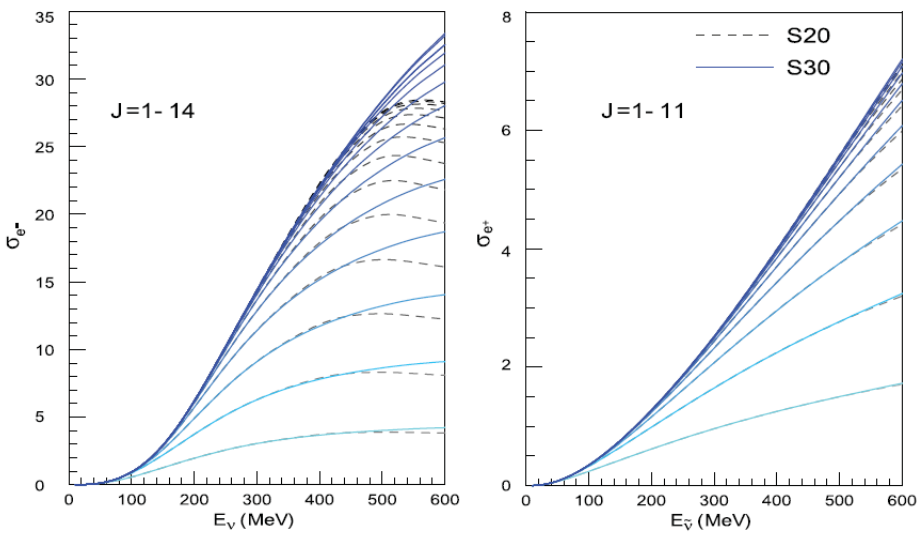

PHYSICAL REVIEW C **83**, 024303 (2011)

RQRPA in ^{12}C

The calculated RQRPA (within *S*30 and *E*2*qp* = 500 MeV) quasielastic (*νe*,12C) cross section per neutron (solid line) is compared with that for the (*νμ*,12C) scattering data measured at MiniBooNE [13]; the dotted line shows the same calculation but renormalized by a factor of 1.5. Also displayed are the calculations done by Martini *et al.* [73,103] within the RFGM for pure (1p-1h) excitations (dashed line) and with the inclusion of the np-nh channels (dot-dashed line).

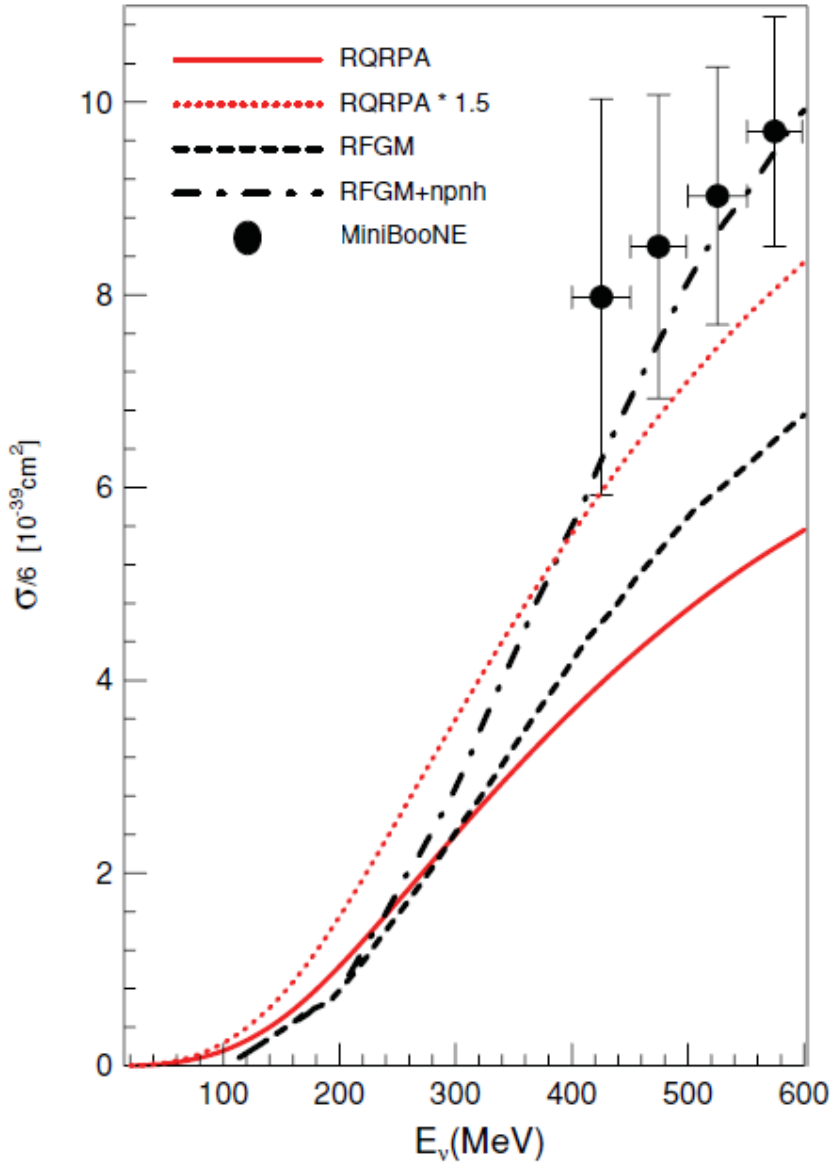

[13] A. A. Aguilar-Arevalo *et al.* (MiniBooNE Collaboration), Nucl. Instrum. Methods A **599**, 28 (2009).
[73] M. Martini, M. Ericson, G. Chanfray, and J. Marteau, Phys. Rev. C **80**, 065501 (2009).
[103] M. Martini, M. Ericson, G. Chanfray, and J. Marteau, Phys. Rev. C **81**, 045502 (2010).

NEUTRINO AND ANTINEUTRINO CHARGE-EXCHANGE . . .

PHYSICAL REVIEW C **83**, 024303 (2011)

QRPA/PQRPA/RQRPA in ^{56}Fe

- ♣ 12 s.p. levels: 2, 3 and 4 ħϖ,
- ♣ 3ħϖ, s.p.e of ^{56}Ni, 2&4 s.p.e. H.O.
- ♣ v^{pair}_s (p,n) to Δ(p,n) experimental.
- ♣ v^{ph}_s =24, v^{ph}_t =64,(MeV.fm^3) G. resonance in ^{48}Ca [NPA572,329(1994)].
- ♣t =2 v^{ph}_t /(v^{pair}_s (p)+ v^{pair}_s (n))=0, B(GT-) =17.7 ~ B(GT-)=18.68 Skyrme [NPA716,230(2003)] overestimates exp. 9.9±2.4 [NPA410,371(1983)].

$$\langle \sigma_e \rangle = \int dE_\nu \sigma(E_\nu) n(E_\nu),$$

$$n(E_\nu) = \frac{96 E_\nu^2}{M_\mu^4}(M_\mu - 2E_\nu),$$

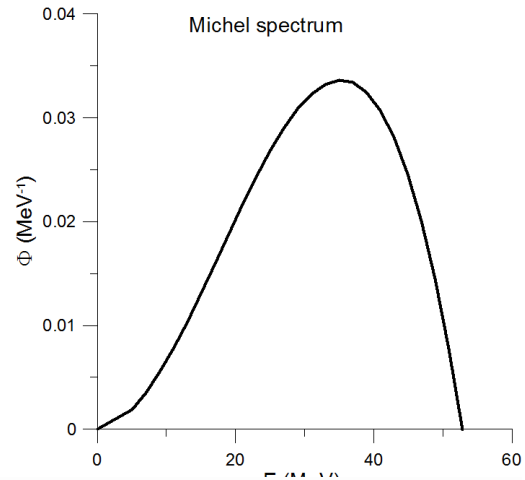

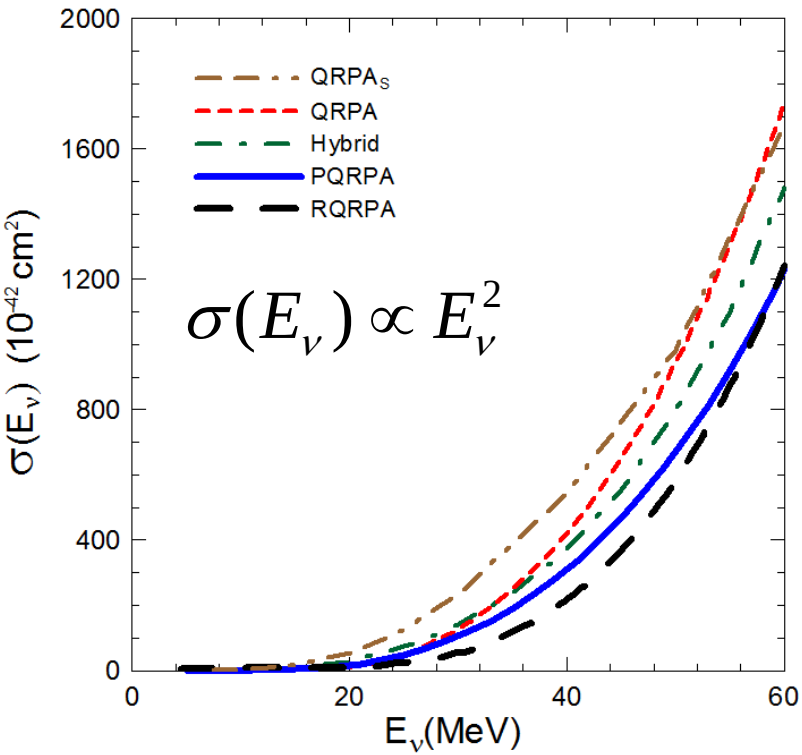

Model	$\langle \sigma_e \rangle$
QRPA	264.6
PQRPA	197.3
Hybrid$^{(a)}$ [14]	228.9
Hybrid$^{(b)}$ [14]	238.1
TM [26]	214
RPA [27]	277
QRPA$_S$ [15]	352
RQRPA [16]	140
Exp[5] **KARMEN**	$256 \pm 108 \pm 43$

A.Samana & C.Bertulani, PRC78, 024312 (2008)

QRPA/PQRPA/RQRPA in ^{56}Fe

Supernovae Neutrinos – To estimate events in supernova detectors.

$$N_e \equiv N_e(T_{\nu_e}) = N_t \int_0^\infty F_e^0(E_\nu, T_{\nu_e})\sigma(E_\nu)\varepsilon(E_\nu)dE_\nu,$$

$$\tilde{N}_e \equiv \tilde{N}_e(T_{\nu_x}) = N_t \int_0^\infty F_x^0(E_\nu, T_{\nu_x})\sigma(E_\nu)\varepsilon(E_\nu)dE_\nu.$$

Effective temperature

Neutrino energy

Time-integrated energy

$$F_\alpha^0(E, T_\alpha, \eta_\alpha = 0, L_\alpha, D) = \frac{L_\alpha}{4\pi D^2 T_\alpha^4 F_3(0)} \frac{E^2}{e^{E/T_\alpha}+1},$$

Distance to supernova

Norm.factor

Pinching parameter

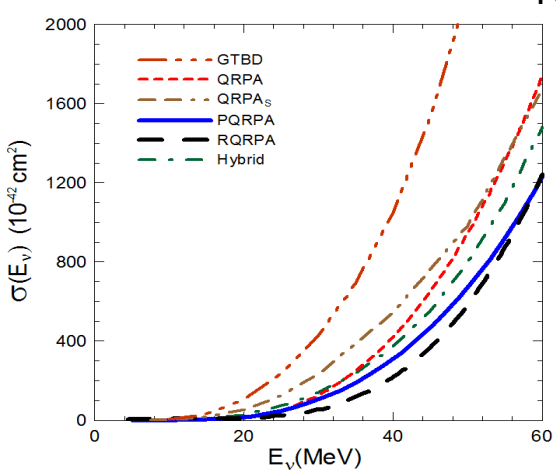

D~ 10 kpc,
$L_\alpha = E_b$. 1/6,
$E_b = 3\times10^{53}$ erg,
$\alpha = \nu_\alpha = \{\nu_e, \nu_\mu, \nu_\tau\}$
$T(\nu_x)/T(\underline{\nu}_e) = 1.5$,
$T(\nu_e)/T(\underline{\nu}_e) = 0.8$,
$T(\underline{\nu}_e) = 5$ MeV

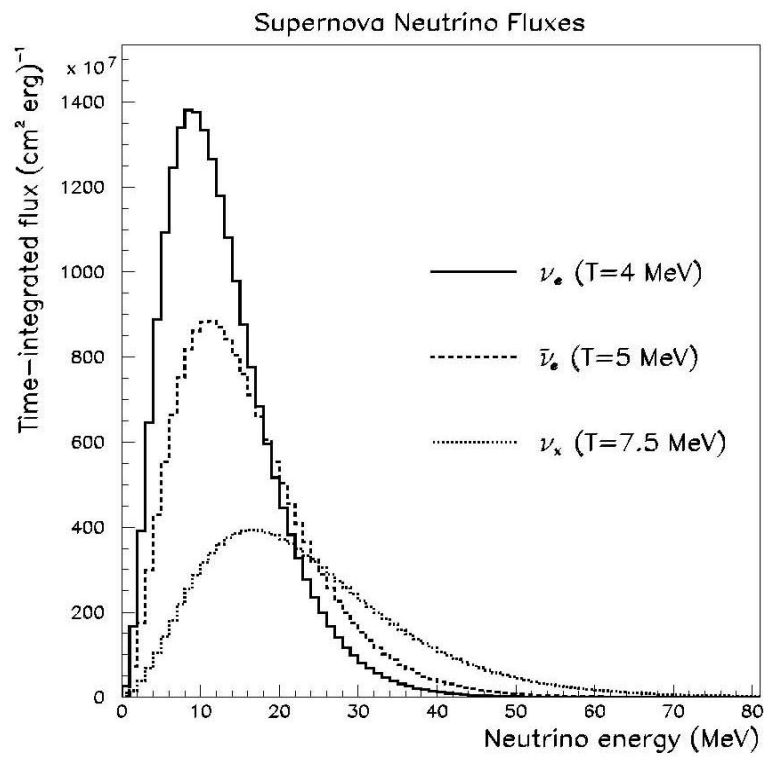

Fig. 1. Neutrino energy spectra at the neutrino-sphere.

QRPA/PQRPA/RQRPA in ^{56}Fe

$$\nu_e + {}^{56}Fe \rightarrow {}^{56}Co^* + e^-$$

A.S.& C.B., PRC 78, 024312 (2008)

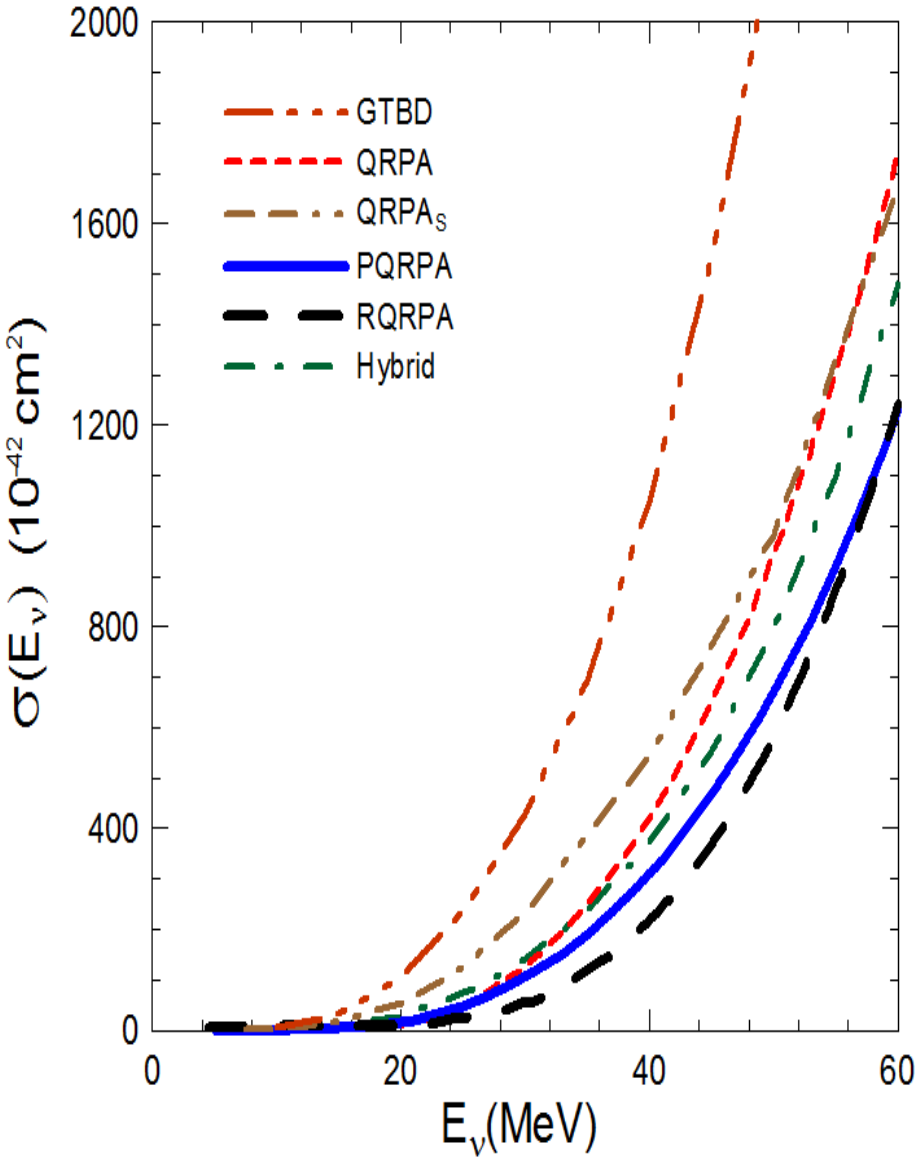

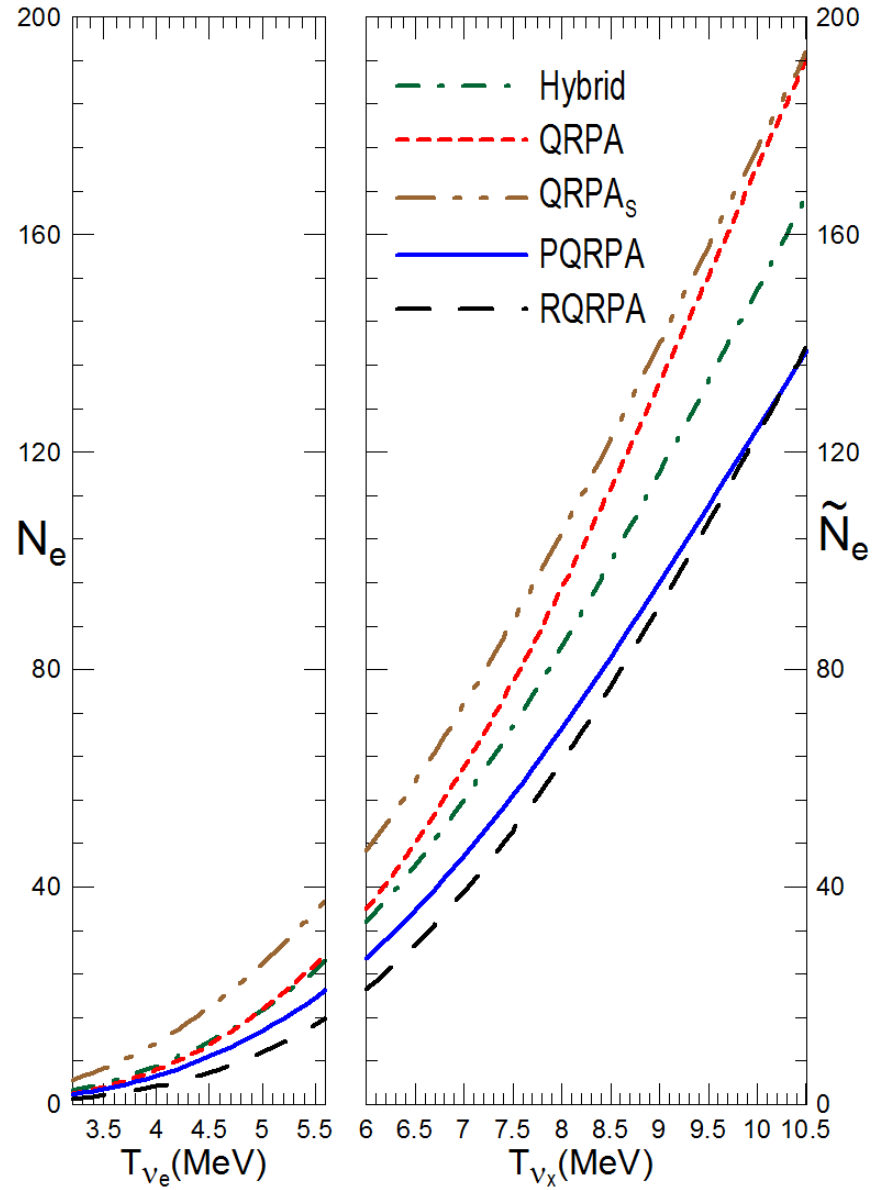

QRPA/PQRPA/RQRPA in ^{56}Fe

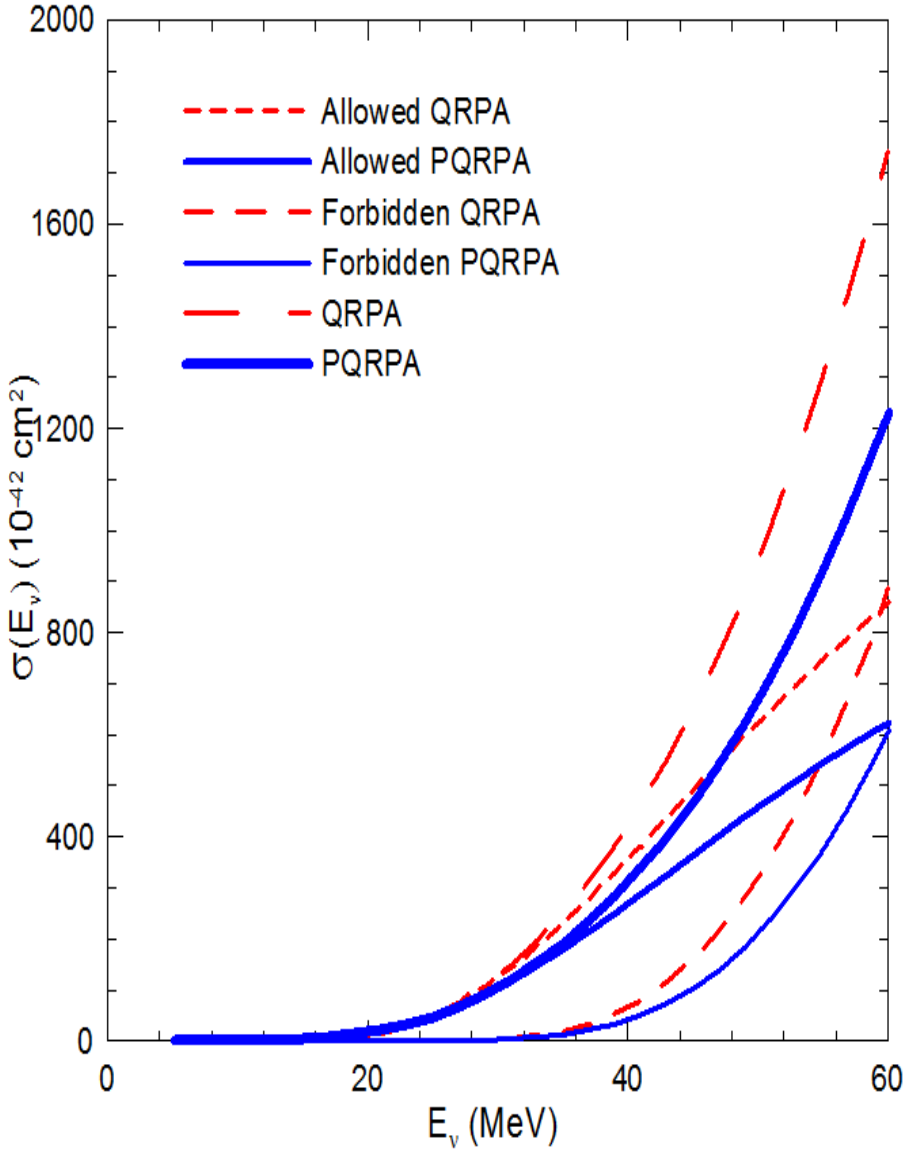

PQRPA & QRPA, PRC 78, 024312 (2008)

RQRPA DD-ME2 , PRC 77,024608 (2008)

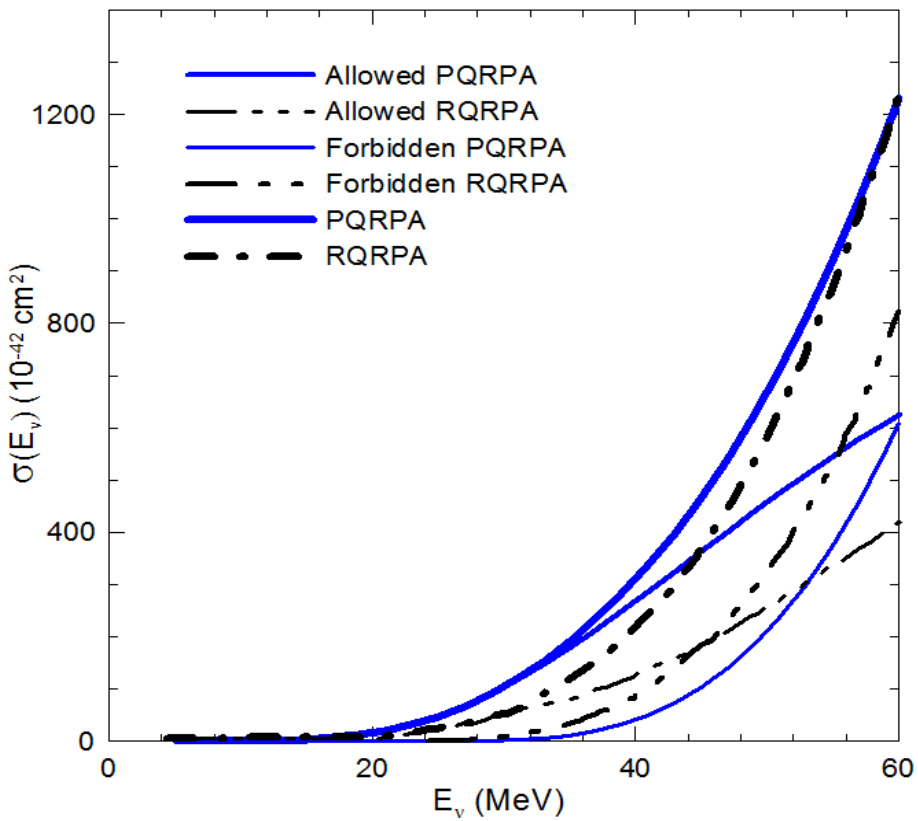

QRPA/PQRPA/RQRPA in ^{56}Fe

RQRPA (N. Paar, private comunication)

J^π	Hybrid$^{(a)}$	Hybrid$^{(b)}$	QRPA	PQRPA	RQPRA		
0^+	45.7	52.7	41.1	56.6			
1^+	112.9	112.1	172.7	108.1			
allowed	158.6	164.8	213.8	164.7	$\sim$ 78.3		
2^+	4.0	4.1	2.9	1.8			
3^+	4.4	4.2	2.5	1.4			
0^-	0.4	0.4	1.1	0.7			
1^-	29.3	29.4	20.7	14.0			
2^-	32.0	35.0	22.4	13.9			
3^-	0.2	0.2	1.2	0.8			
Forbidden	70.3	73.3	50.8	32.6	$\sim$ 61.4		
Total	228.9	238.1	264.6	197.3	140.0	360	257
256± 116 KARMEN	$g_A \sim 0.93$		$g_A = 1.0$		$g_A \sim 0.9$	g_A=1.262	g_A=1.0

PQRPA/RQRPA in ^{56}Fe

PQRPA (δ-force) and RQRPA (DD-ME2)

PQRPA [PRC78, 024312(2008)]
RQRPA (N. Paar, private com. 05-29-09)

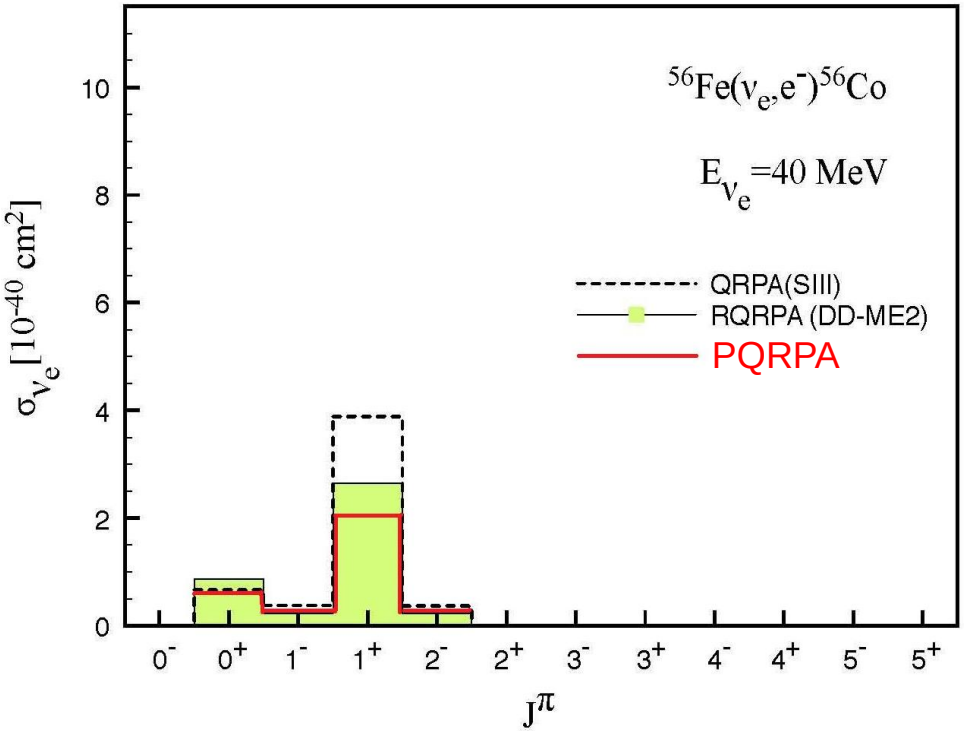

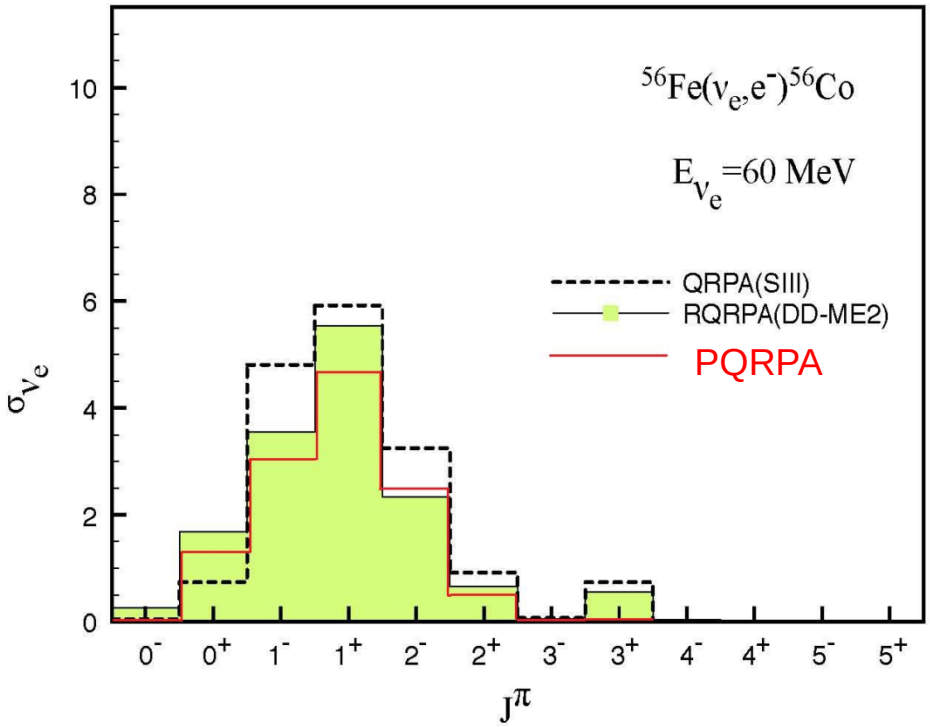

QRPA/RQRPA in ^{56}Fe

MODELING NUCLEAR WEAK-INTERACTION PROCESSES WITH RELATIVISTIC ENERGY DENSITY FUNCTIONALS
N. PAAR, T. MARKETIN, D. VALE, D. VRETENAR, http://arxiv.org/abs/1505.07486v1

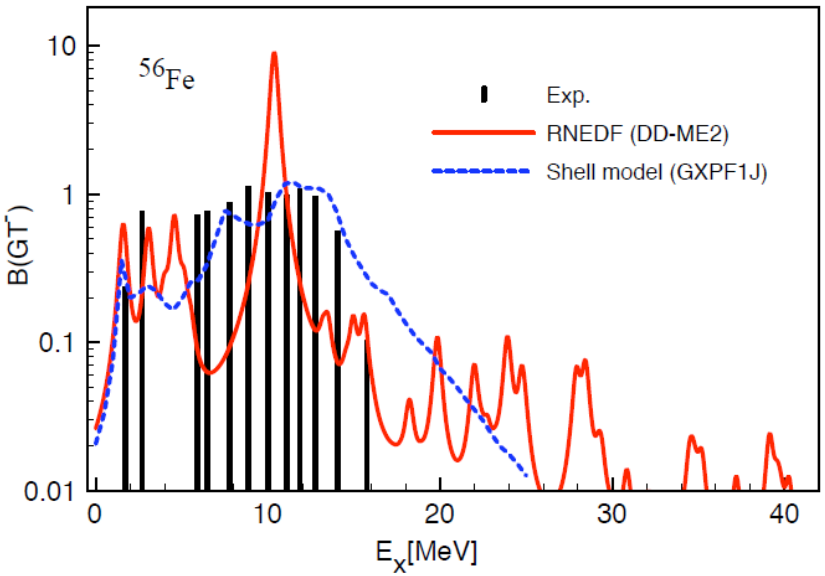

The Gamow-Teller (GT−) transition strength distribution for ^{56}Fe, shown as a function of excitation energy in the final nucleus. The RQRPA results based on the RNEDF DD-ME2 are compared to the shell model calculations (GXPF1J),[28] and available data from (p, n) reactions.[39]

Gamow-Teller (GT−) strength distributions for ^{18,20,22}O calculated with the RHB+RQRPA model (DD-ME2 functional and Gogny pairing in the T = 1 channel). The strength of the T = 0 particle-particle interaction Eq. (1) varies from V_0 = 0 to V_0 = 300 MeV.

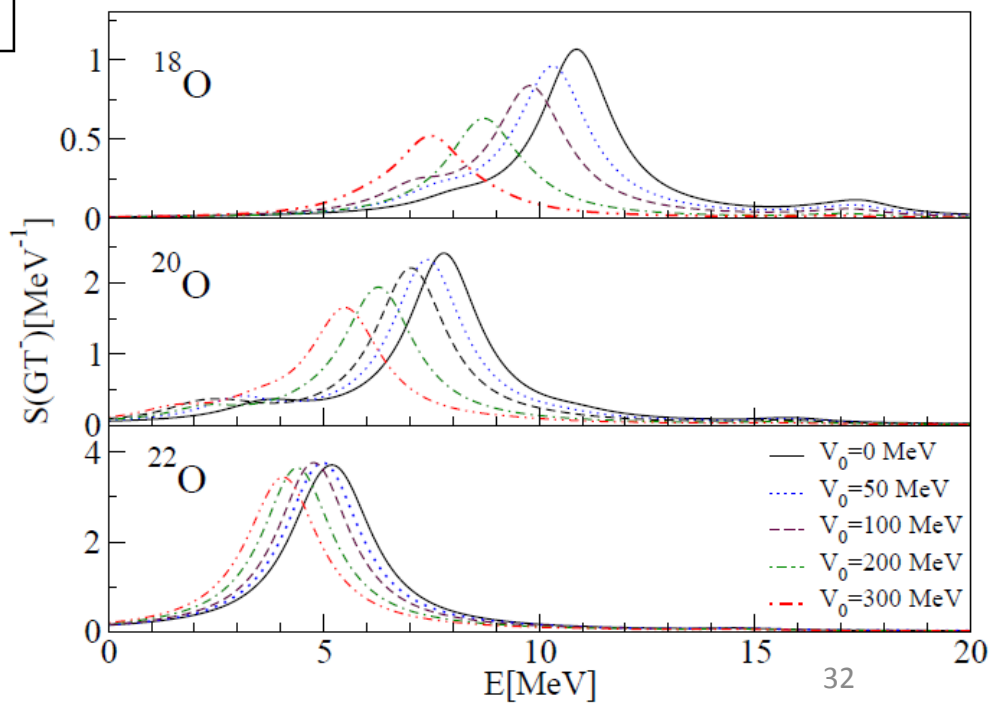

QRPA & RQRPA systematic calculations

Muon capture rates within the projected QRPA
Danilo Sande Santos, Arturo R. Samana, Francisco Krmpotic, Alejandro J. Dimarco
http://pos.sissa.it/archive/conferences/142/120/XXXIV%20BWNP_120.pdf
Ratios of theoretical to experimental inclusive muon capture rates for different nuclear models, as function of the mass number *A*. The present QRPA and PQRPA results, as well as the RQRPA calculation [13] were done with *g*A = 1.135, while in the RPA+BCS model [11] was used the unquenched value *g*A = 1.26 for all multipole operators, except for the GT ones where it was reduced to *g*A ~ 1.

(^{12}C, ^{20}Ne, ^{24}Mg, ^{28}Si, ^{40}Ar, ^{52}Cr, ^{54}Cr, ^{56}Fe)

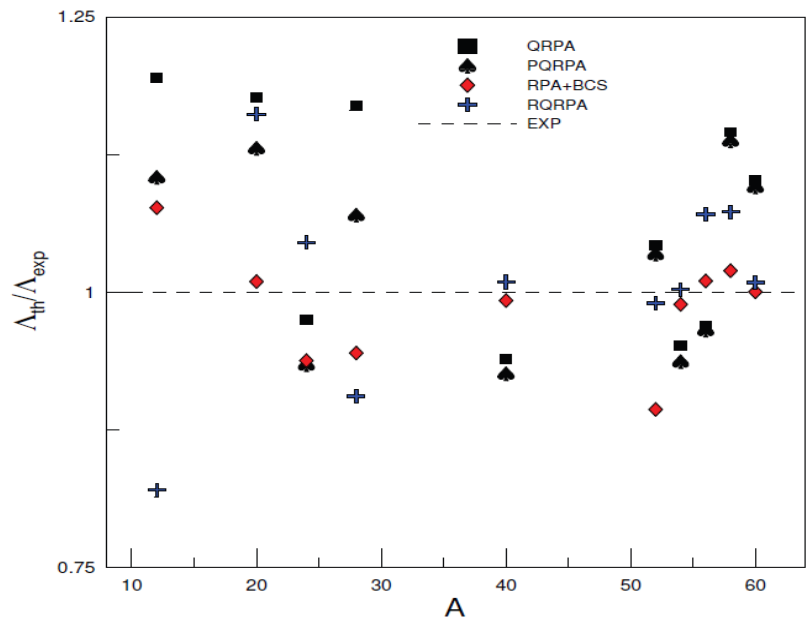

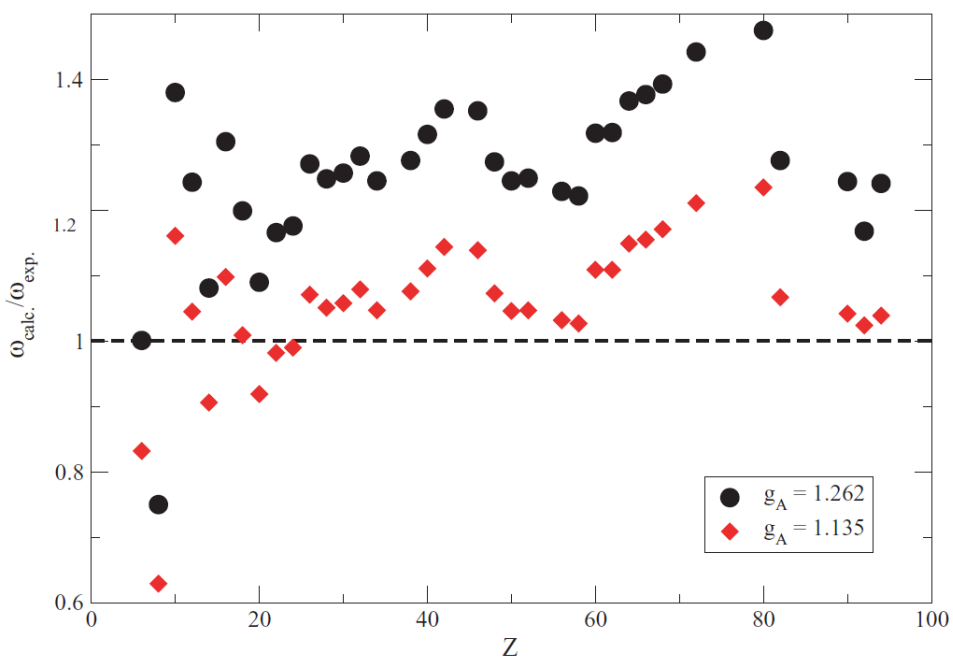

Relativistic quasiparticle random-phase approximation calculation of total muon capture rates, T. Marketin, N. Paar, T. Nikˇsi´c, and D. Vretenar, PHYSICAL REVIEW C **79**, 054323 (2009)
Ratio of the calculated and experimental total muon capture rates, as function of the proton number *Z*. Circles correspond to rates calculated with the free-nucleon weak form factors Eqs. (10)–(13) [21], and diamonds denote values obtained by quenching the free nucleon axial-vector coupling constant *gA* =1.262 to *gA* = 1.135 for all operators, i.e., in all multipole channels.

QRPA & RQRPA systematic calculations

MODELING NUCLEAR WEAK-INTERACTION PROCESSES WITH RELATIVISTIC ENERGY DENSITY FUNCTIONAS
N. PAAR, T. MARKETIN, D. VALE, D. VRETENAR, http://arxiv.org/abs/1505.07486v1

RHB+RQRPA (DD-ME2) inclusive neutrino-nucleus cross sections averaged over the Fermi-Dirac distribution for T = 4 MeV, _ = 0, as a function of the mass number of target nuclei. The cross sections for particular groups of target nuclei are further marked with filled (red) circles for stable nuclei, crosses for nuclei with N/Z < 1, and filled (blue) squares for nuclei with N/Z > 1.5.

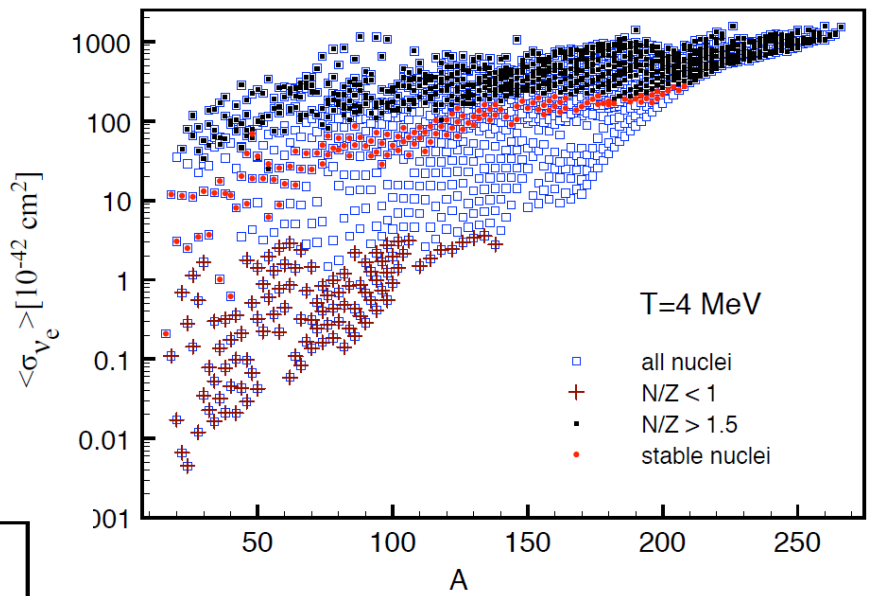

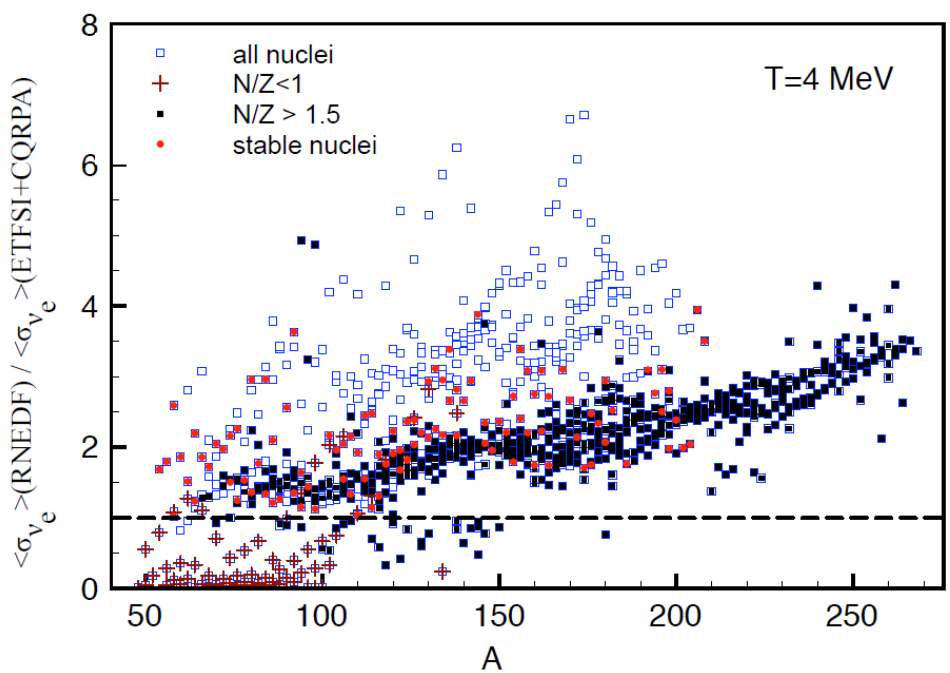

The ratio of the RHB+RQRPA cross sections shown in Fig. 8 and the cross sections calculated using the ETFSI+CQRPA framework.

ETFSI+CQRPA : N. Borzov and S. Goriely, *Phys. Rev. C 62 (2000) 035501*

ν-40 Ar Cross section

LArTPC - Liquid **Ar**gon **T**ime **P**rojection **C**hambers

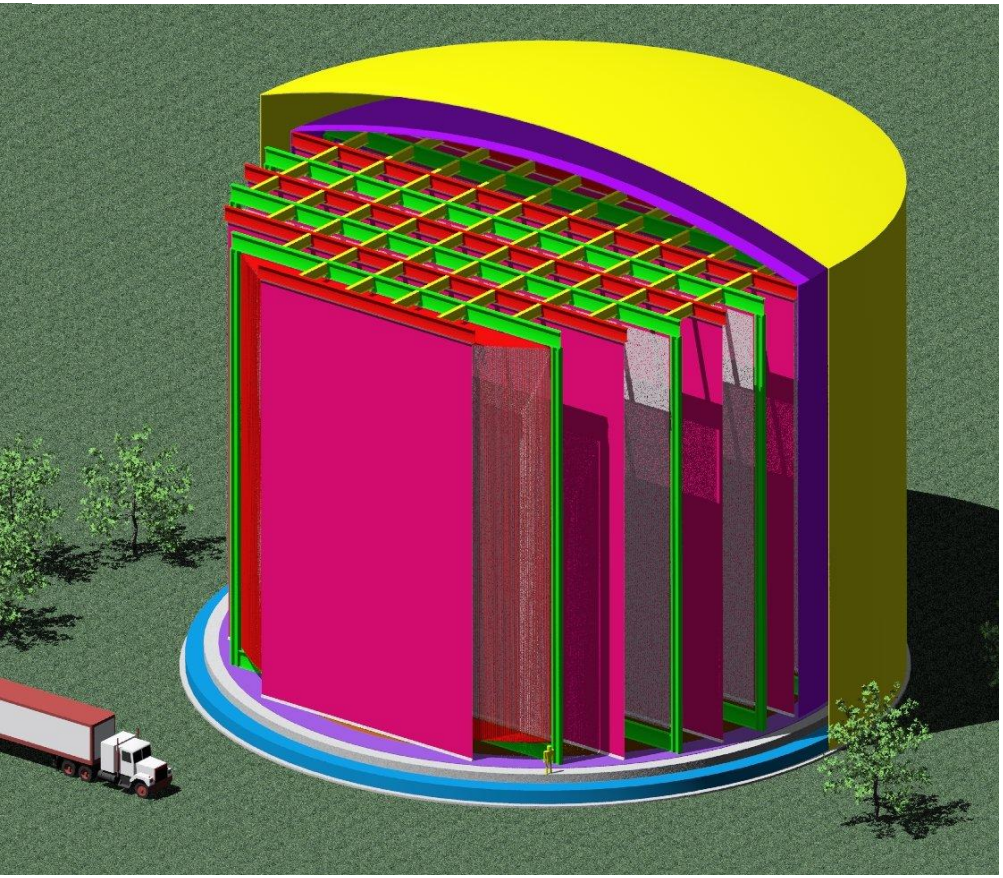

http://www-lartpc.fnal.gov/

SM - T. Suzuki & M. Honma,
arXiv:1211.4078v1 [nucl-th] 17 Nov 2012

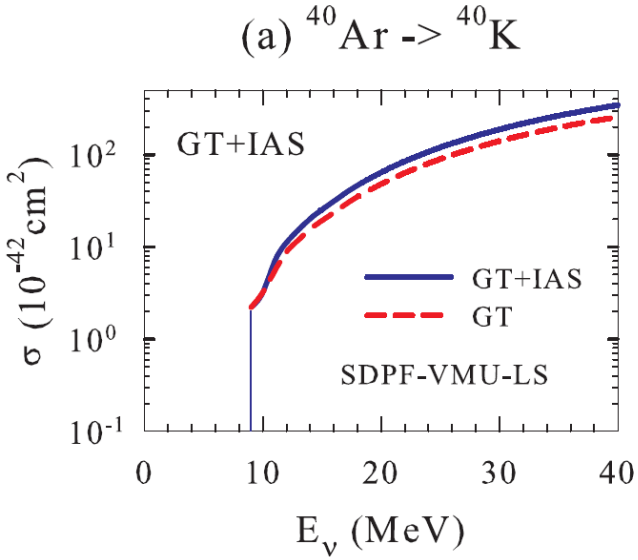

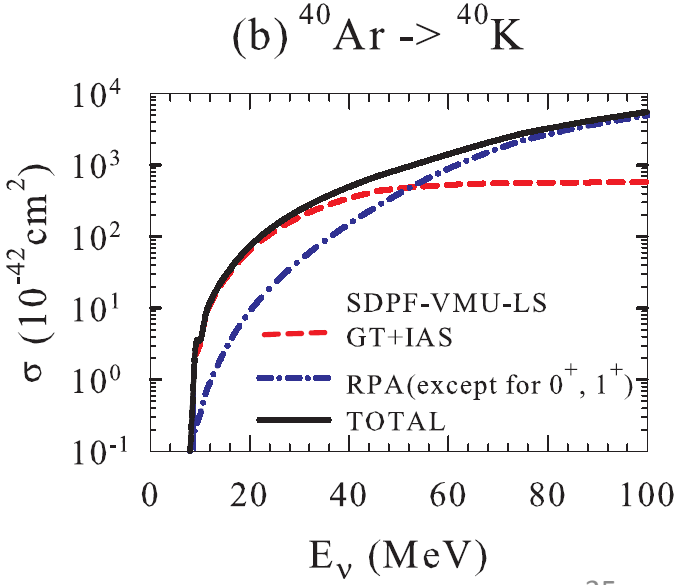

ν-^{16}O Cross section

in work

(S. Santana & A. Samana)

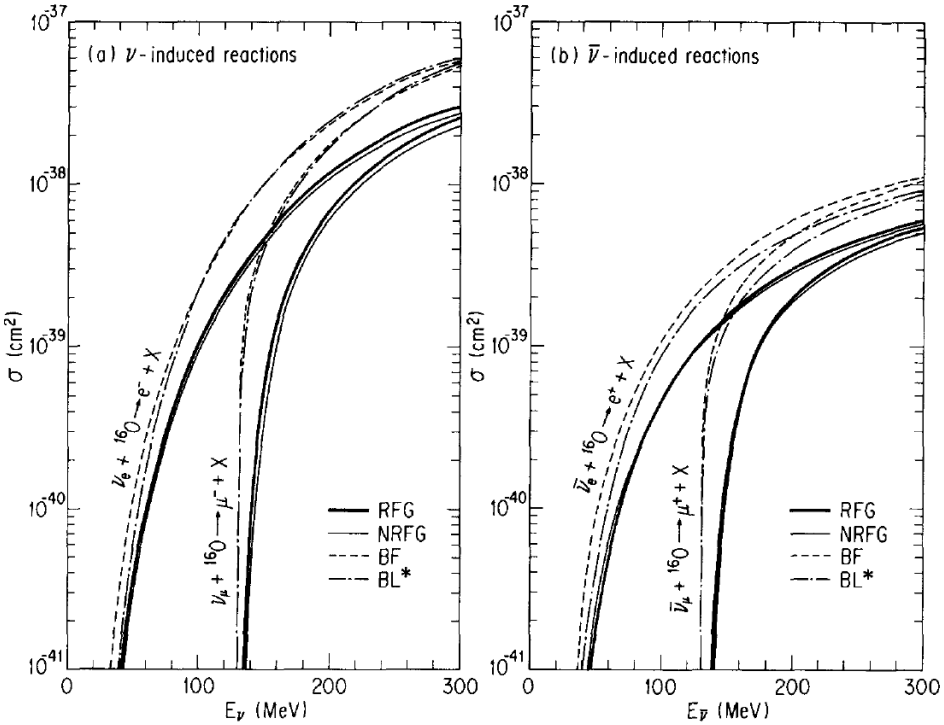

Neutrino/antineutrinno electronic and muonic 16O cross section as function of neutrino/ antineutrino energy.

T. KURAMOTO, M. FUKUG1TA, Y. KOHYAMA and K. KUBODERA, Nuclear Physics A512 (1990) 711

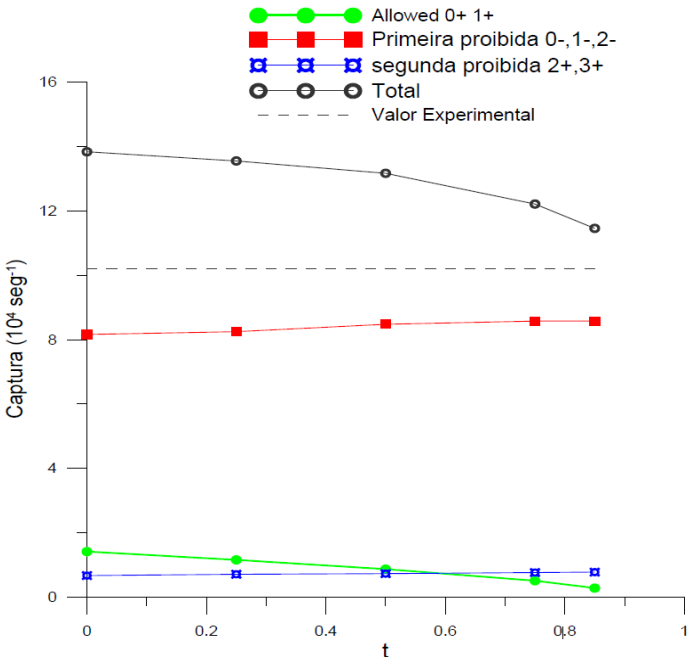

QRPA-based muon capture inclusive rates as function of particle-particle chanel in δ-interaction.

ν-^{16}O Cross section

in work (S. Santana & A. Samana)

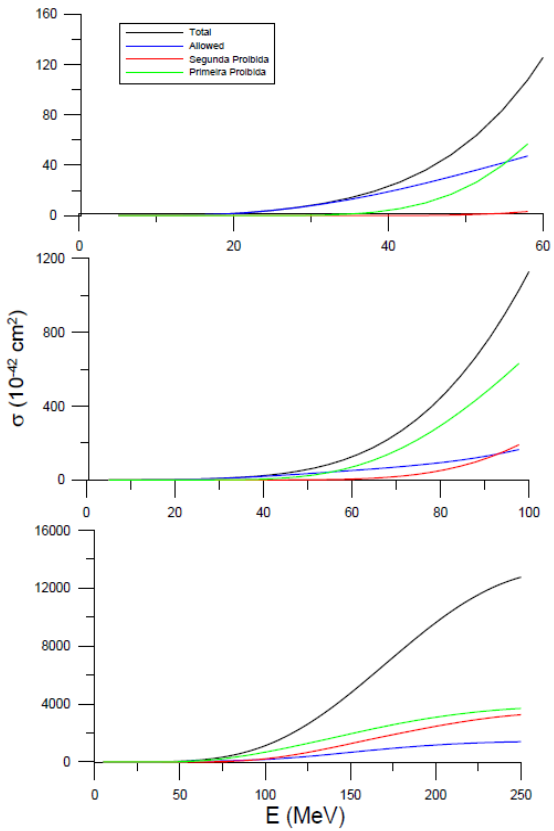

QRPA-based neutrino cross section as function of neutrino energy.

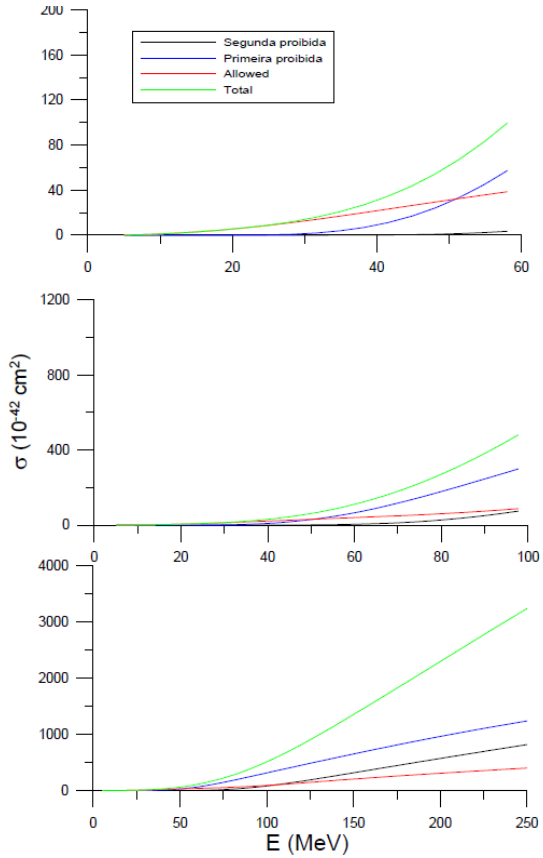

QRPA-based antineutrino cross section as function of antineutrino energy.

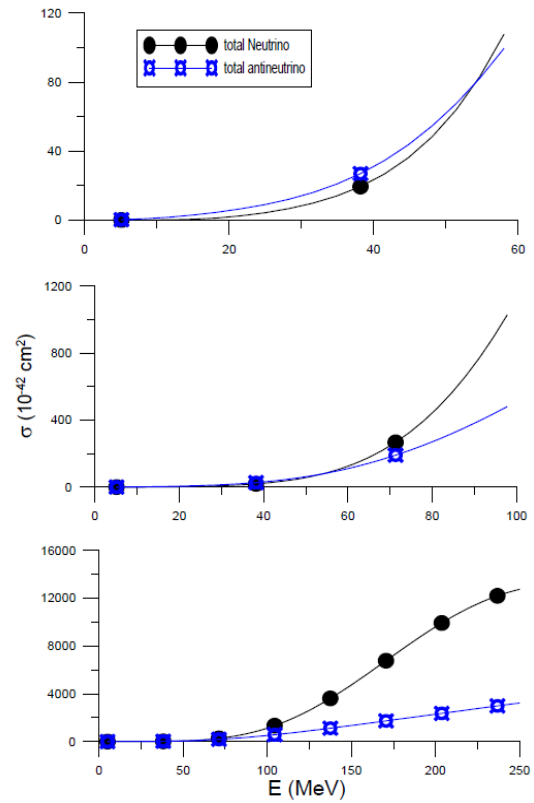

QRPA-based neutrino/antineutrino cross section as function of neutrino /antineutrino energy.

QRPA calculations for Double Beta Decay

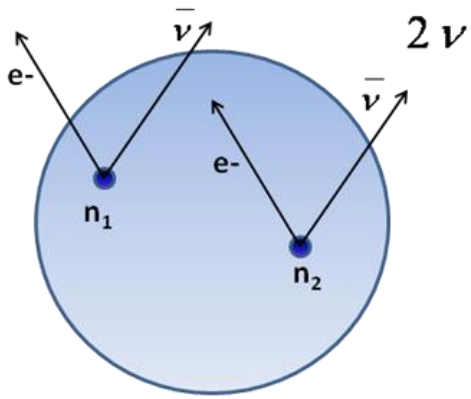

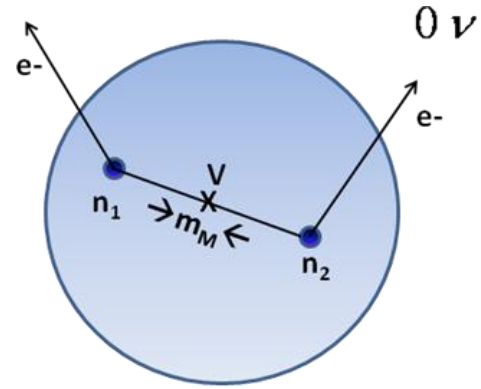

$$(A,.Z) \rightarrow (A, Z+1) + e^- + \bar{\nu}$$
$$\rightarrow (A, Z+2) + 2e^- + 2\bar{\nu}$$

$$(A,.Z) \rightarrow (A, Z+1) + e^- + \bar{\nu} \equiv (A, Z+1) + e^- + \nu$$
$$\rightarrow (A, Z+2) + 2e^-$$

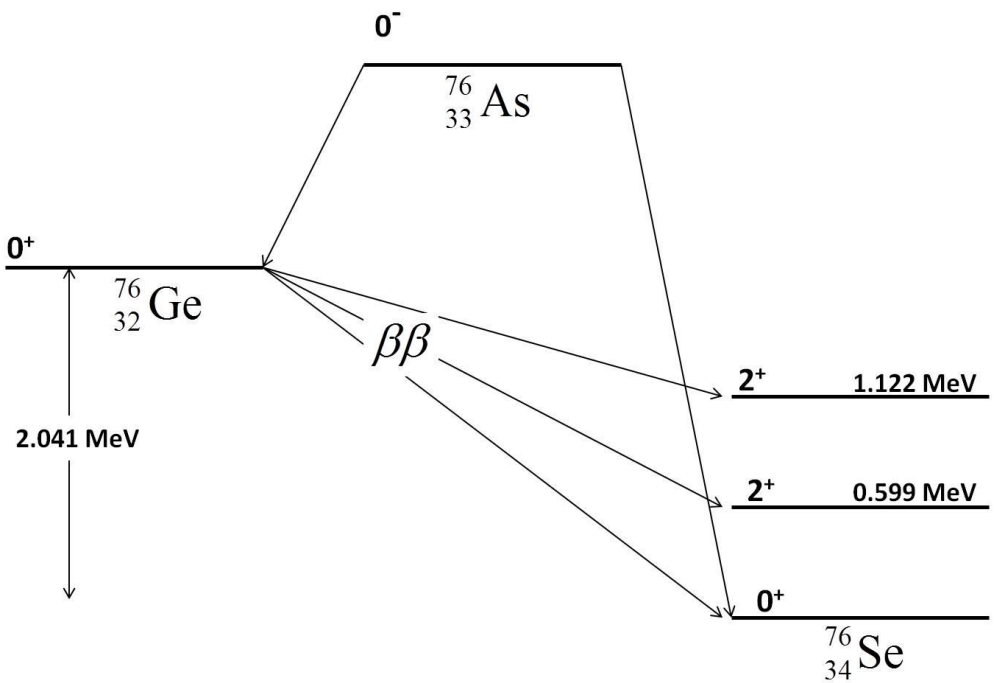

$$T_{2\nu}^{-1} = G_{2\nu} M_{2\nu}^{2}$$

$$T_{2\nu}^{-1} = G_{0\nu} M_{0\nu}^{2} \langle m_\nu \rangle^2$$

QRPA calculations for Double Beta Decay

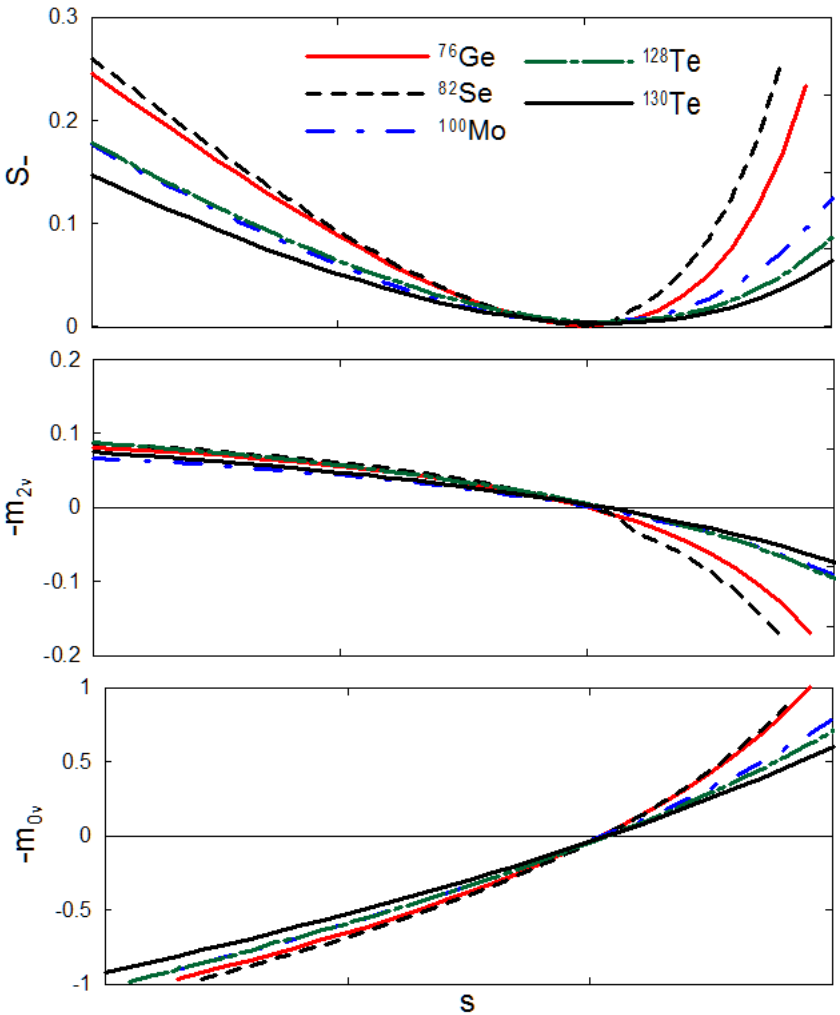

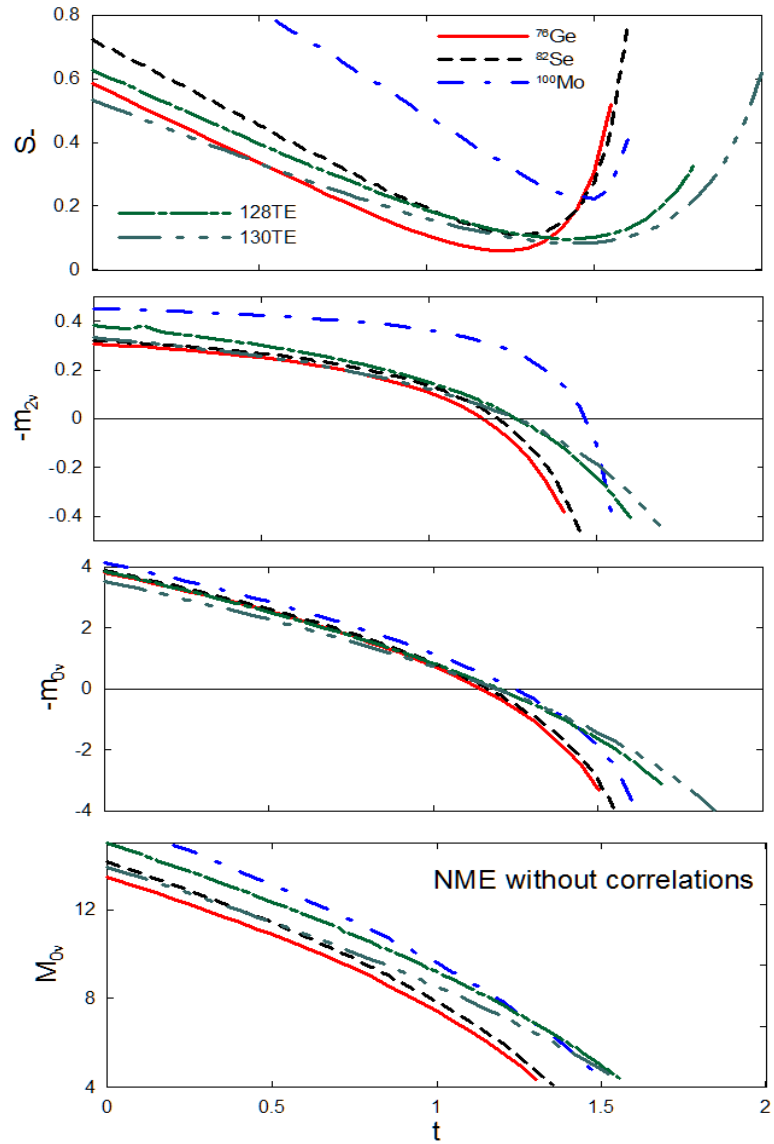

NME and weak observables type Fermi as function of *s* parameter and type Gamow Teller as function of *t* parameter.

QRPA calculations for Double Beta Decay

QRPA NME (in MeV^{-1}) as function of as function of nuclear spins $J^{\pi}= 0\pm$ to $10\pm$ for $0\nu\beta\beta$.

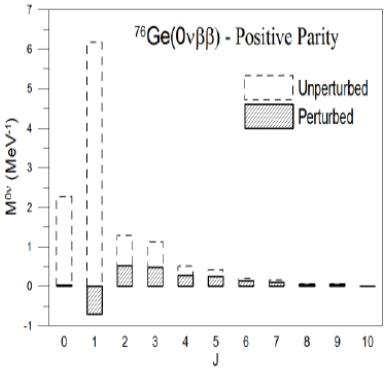

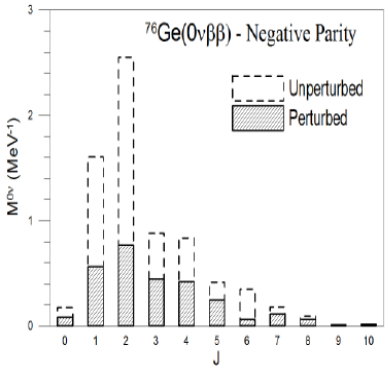

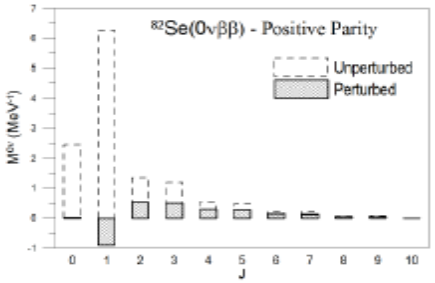

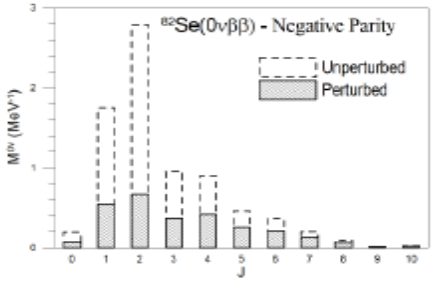

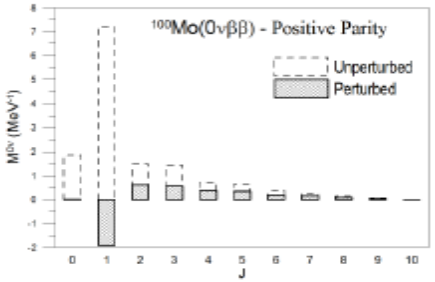

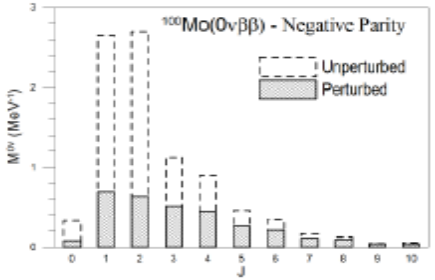

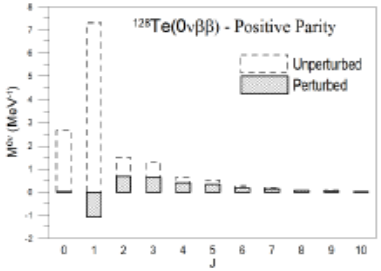

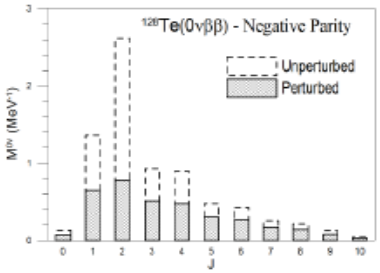

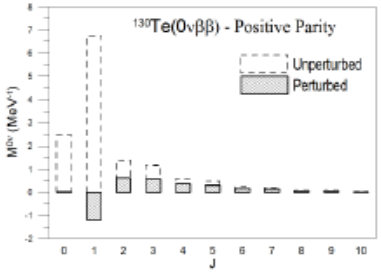

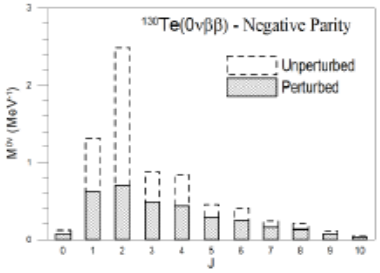

Computer code for double beta decay QRPA based calculations, C. A. Barbero, F. Krmpotić, A. Mariano, A. R. Samana, V. dos Santos Ferreira, and C. A. Bertulani, AIP Conference Proceedings 1625, 169 (2014); doi: 10.1063/1.4901786

FQTDA calculations for Double Beta Decay

$$T_{2\nu}^{-1} = G_{2\nu} M_{2\nu}^{2}$$

$$T_{0\nu}^{-1} = G_{0\nu} M_{0\nu}^{2} \langle m_{\nu} \rangle^{2}$$

$$M_{2\nu}(f) = \sum_{\lambda=0,1} (-)^{\lambda} \sum_{\alpha} \left[\frac{\langle 0_f^+ \| O_\lambda^{\beta-} \| \lambda_\alpha^+ \rangle \langle \lambda_\alpha^+ \| O_\lambda^{\beta-} \| 0^+ \rangle}{D_{\lambda_\alpha^+, f}} \right] \equiv M_{2\nu}^{F}(f) + M_{2\nu}^{GT}(f)$$

	TDA	QTDA	Equações
Ground State [Gs.]	$\lvert HF \rangle$	$\lvert BCS \rangle$	HF / BCS
Intermediate State	$a_p^\dagger a_n \lvert HF \rangle$	$\alpha_n^\dagger \alpha_p \lvert BCS \rangle$	TDA / QTDA
Final State	$a_p^\dagger a_p^\dagger a_n a_n \lvert HF \rangle$	$\alpha^\dagger \alpha^\dagger \alpha^\dagger \alpha^\dagger \lvert BCS \rangle$	FTDA / FQTDA
Interação-δ	$V = -4\pi(v_s P_s + v_t P_t)\delta(r)$		

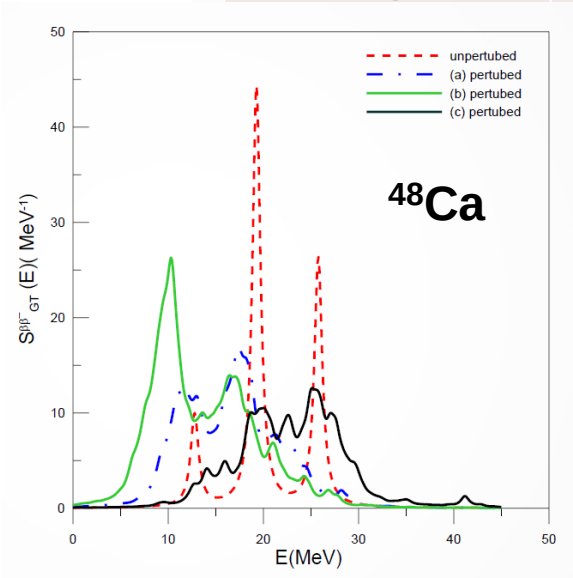

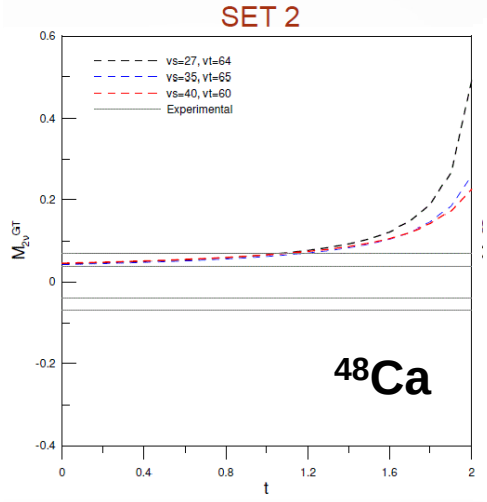

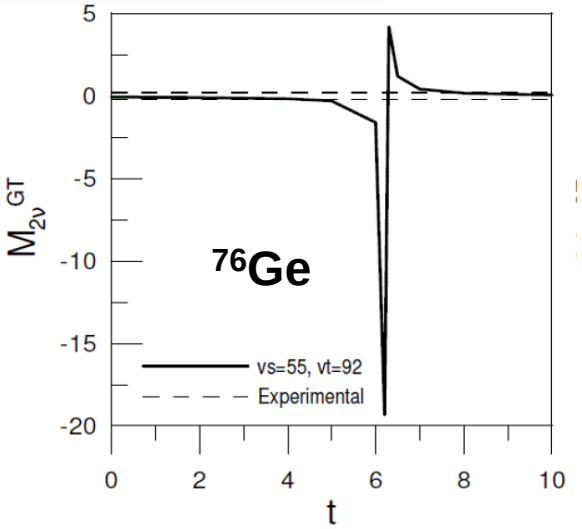

Four **Q**uasiparticle **T**amm-**D**amcoff **A**pproximation (FQTDA)
L. de Oliveira; A.R. Samana, F. Krmpotic, A.E. Mariano, C.A. Barbero
Journal of Physics: Conference Series 630 (2015) 012048

On neutrino-nucleon calculations

Neutrinos generating events for intranuclear cascade in CRISP code
(D. Oliva in poster session)

CRISP ?

Colaboration **R**io de Janeiro **I**lhéus **S**ão **P**aulo

MCMC

Multi - **C**olisional **M**onte **C**arlo

Intranuclear Cascate

MCEF

Monte **C**arlo **E**vaporation **F**ission

Nuclear evaporation/Fission

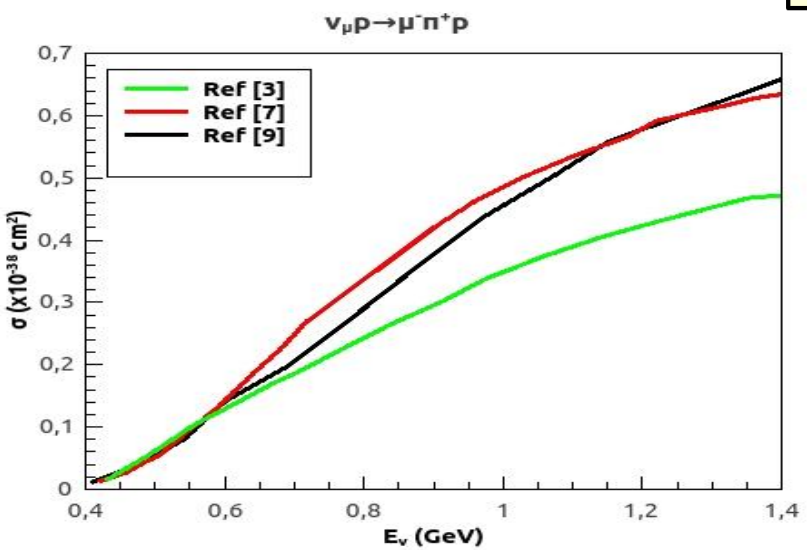

	Ref [3]	Ref[7]	Ref[9]
a_0	-0.92462	2.67268	1.05155
a_1	5.04353	-19.06087	-8.45383
a_2	-11.59230	51.24583	25.33257
a_3	15.70827	-66.79729	-37.05122
a_4	-11.57894	47.22928	30.65338
a_5	4.34806	-17.44865	-13.54899
$'a_6$	-0.65715	2.64360	2.46629

[3] C. Barbero et. al., Phys. Lett. B664 (2008) 70
[7] Tina J. Leitner, PhD Thesis, September 2005, Institut fur Theoretische Physik Justus-Liebig-Universit t Gießen
[9] G. P. Zeller (Fermilab) ,Phys. Rev. D86, 010001 (2012) 436-438.

Total cross sections of the $\nu_\mu p \rightarrow \mu^- \pi^+ p$ scattering processes from Ref. [3,7,9] adjusted to $\sigma(E_\nu) = \sum_n^N a_n E_\nu^n$

Numerical tool: **Q**uasiparticle **R**andom **Ap**proximation

QRAP * **code** (open source)

Single particle States,.
1 to 6 ħϖ H.O.

$$(e_t - \lambda_t)(u_t^2 - v_t^2) + u_t v_t \Delta_t = 0,$$

$$\left\langle BCS \,|\, \hat{N} \,|\, BCS \right\rangle = \sum_{t=n(p)} (2j_t + 1) v_t^2 = N(Z)$$

QRPA

$$\begin{pmatrix} \mathcal{A} & \mathcal{B} \\ \mathcal{B} & \mathcal{A} \end{pmatrix} \begin{pmatrix} X \\ Y \end{pmatrix} = \omega \begin{pmatrix} X \\ -Y \end{pmatrix},$$

$$V = -4\pi \left(v_s P_s + v_t P_t\right) \delta(r),$$

PQRPA

$$2\hat{e}_p u_p v_p - \Delta_p (u_p^2 - v_p^2) = 0,$$

$$\begin{pmatrix} \mathcal{A}_\mu & \mathcal{B} \\ -\mathcal{B}^\dagger & -\mathcal{A}^*_{-\mu} \end{pmatrix} \begin{pmatrix} \mathcal{X}_\mu \\ \mathcal{Y}_\mu \end{pmatrix} = \Omega_\mu \begin{pmatrix} \mathcal{X}_\mu \\ \mathcal{Y}_\mu \end{pmatrix},$$

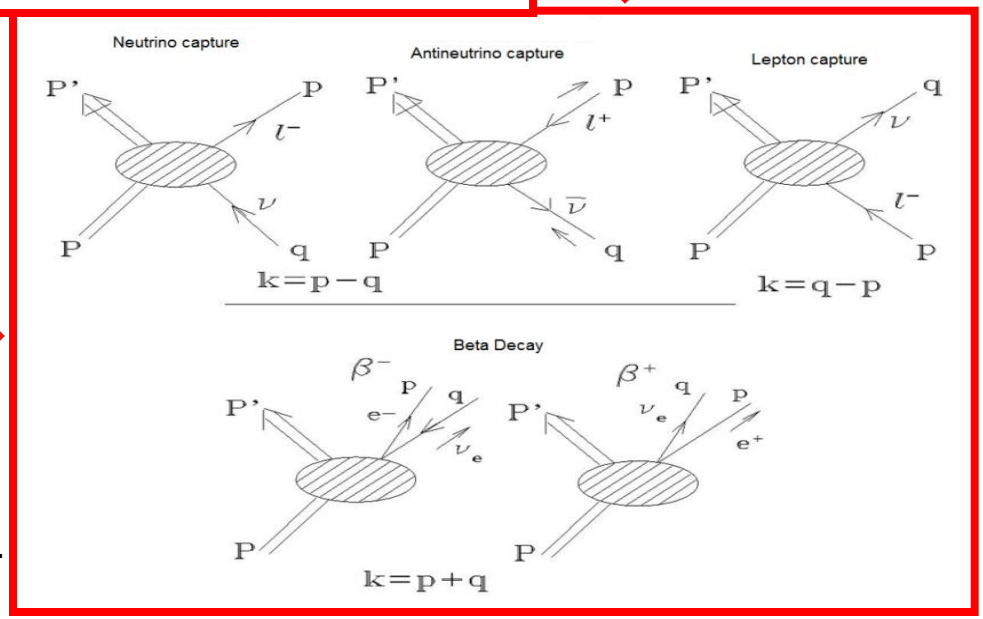

A. R. Samana, F.Krmpotic, and C.A. Bertulani, Comput. Phys. Commun. 181, 1123 (2010)

"QRAP-2B v0.0" Code

Single particle States,.
1 to 6 ħϖ H.O.

QRAP

BCS

$$(e_t - \lambda_t)(u_t^2 - v_t^2) + u_t v_t \Delta_t = 0,$$

$$\left\langle BCS \,|\, \hat{N} \,|\, BCS \right\rangle = \sum_{t=n(p)} (2j_t + 1) v_t^2 = N(Z)$$

Delta interaction

$$V = -4\pi \left(v_s P_s + v_t P_t \right) \delta(r)$$

$$\begin{pmatrix} \mathcal{A} & \mathcal{B} \\ \mathcal{B} & \mathcal{A} \end{pmatrix} \begin{pmatrix} X \\ Y \end{pmatrix} = \omega \begin{pmatrix} X \\ -Y \end{pmatrix},$$

QRPA

0νββ

$$n_1 \to p_1 + e_1 + \bar{\nu}_1$$
$$n_2 + \nu \to p_2 + e_2 \,(\text{if } \nu = \bar{\nu})$$
$$2n \to 2p + 2e$$

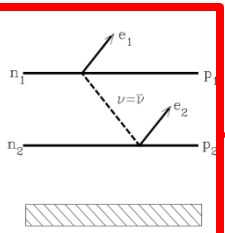

2νββ

$$n_1 \to p_1 + e_1 + \bar{\nu}_1$$
$$n_2 \to p_2 + e_2 + \bar{\nu}_2$$
$$2n \to 2p + 2e + 2\bar{\nu}$$

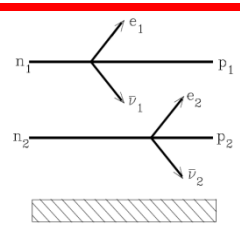

0νββ+Majoron

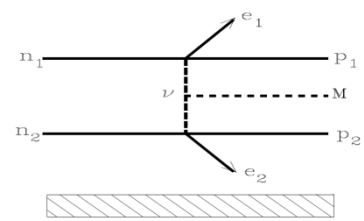

Global Models – Gross Theory of Beta Decay

- Nucleosynthesis of heavy elements in stellar reaction takes place in regions far away of β-stability line, in these regions there exist very few (or not) experimental data.

- Great number of nuclei involved in the reactions:

p-process ~ 2000 nuclei (γ,n),(γ,p),(γ, α),n-,p-, μ-cap, β+

s-process ~ 400 nuclei (n,γ), β-, EC

α-process ~1000 nuclei n-,p-, ν-capture, photodissociation

r-process ~ 4000 nuclei (n,γ),(γ,n), β-, βdn, α-decay,fission.

New Journal of Physics
The open-access journal for physics

The gross theory model for neutrino-nucleus cross-section

A R Samana[1,2], C A Barbero[3,4,8], B Duarte[2], A J Dimarco[5] and F Krmpotić[2,6,7]

$$\lambda_\beta \approx \frac{G^2}{2\pi^3}\int_{-Q_\beta}^{0}\{g_V^2\,|M_F(E)|^2 + g_A^2\,|M_{GT}(E)|^2\}\,f(-E)dE$$

$$|M_\Omega(E)|^2 = \int D_\Omega(E,\varepsilon)W(E,\varepsilon)\frac{dn_1}{d\varepsilon}d\varepsilon$$

A. R. Samana et al, New Journal of Physics 10,033007 024312 (2008)

Global Models – Gross Theory of Beta Decay

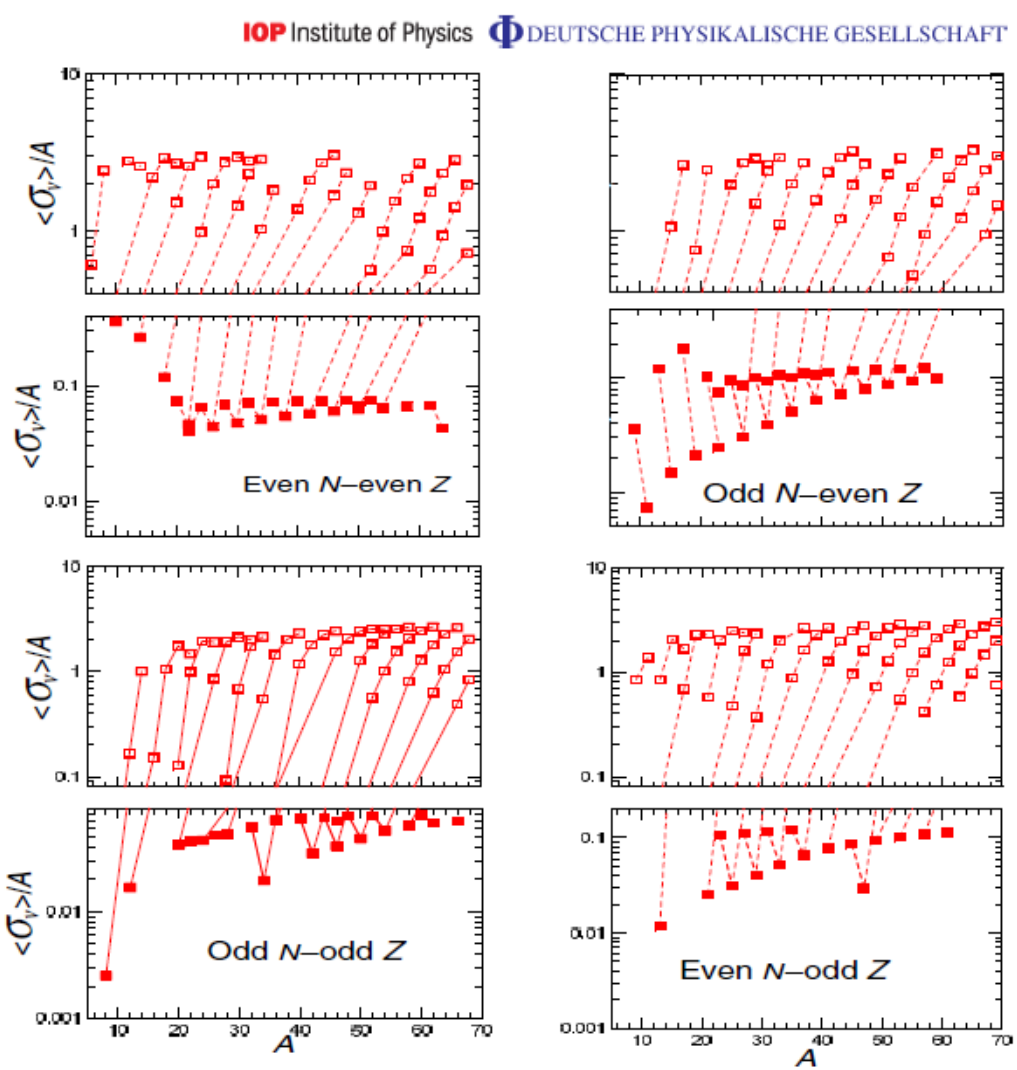

PROCESSO (N-Z)	e-e	e-o	o-o	o-e
β^-	139	191	235	181
C.E	156	198	194	204

$$\sigma(E) = A_0 + A_1 E + A_2 E^2 + A_3 E^3 + A_4 E^4$$

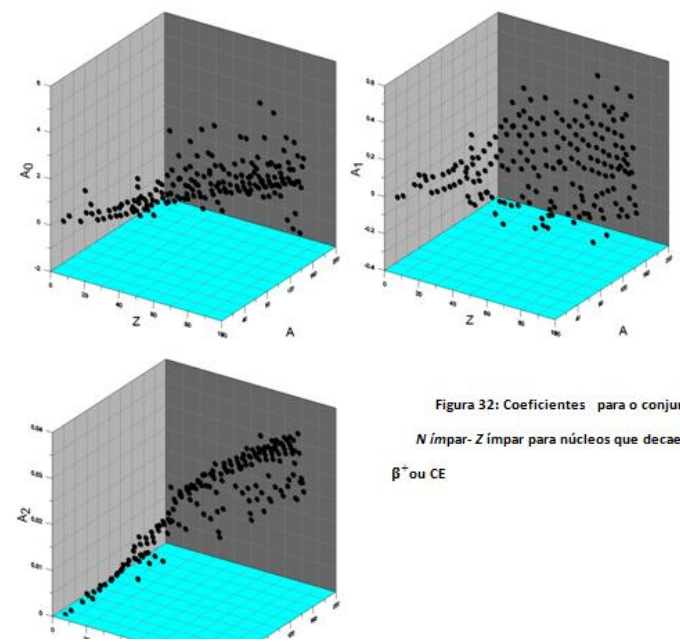

Figura 32: Coeficientes para o conjunto de *N ímpar- Z ímpar* para núcleos que decaem por β^+ou CE

A. R. Samana et al, New Journal of
B. Physics 10,033007 024312 (2008)

M. Cassiano & A. R. Samana,
Master Thesis PROFISICA-UESC 2013

Global Models – Gross Theory of Beta Decay

Weak decay processes in pre-supernova core evolution within the Gross Theory

$$\lambda_{BD}(E,\rho,T,Y_e) = P(0)\int_{-Q}^{0}[\mathcal{G}_F D_F(E) + 3\mathcal{G}_{GT} D_{GT}(E)] \times N\left[1-\left(1-\frac{Q+E}{\epsilon_F}\right)^{\frac{3}{2}}\right] f(-E,\rho,T,Y_e)dE.$$

$$\lambda_{EC}(E,\rho,T,Y_e) = P(0)\int_{-Q}^{\mathcal{E}_F}[\mathcal{G}_F D_F(E) + 3\mathcal{G}_{GT} D_{GT}(E)] \times Z\left[1-\left(1-\frac{Q+E}{\epsilon_F}\right)^{\frac{3}{2}}\right] g(-E,\rho,T,Y_e)dE.$$

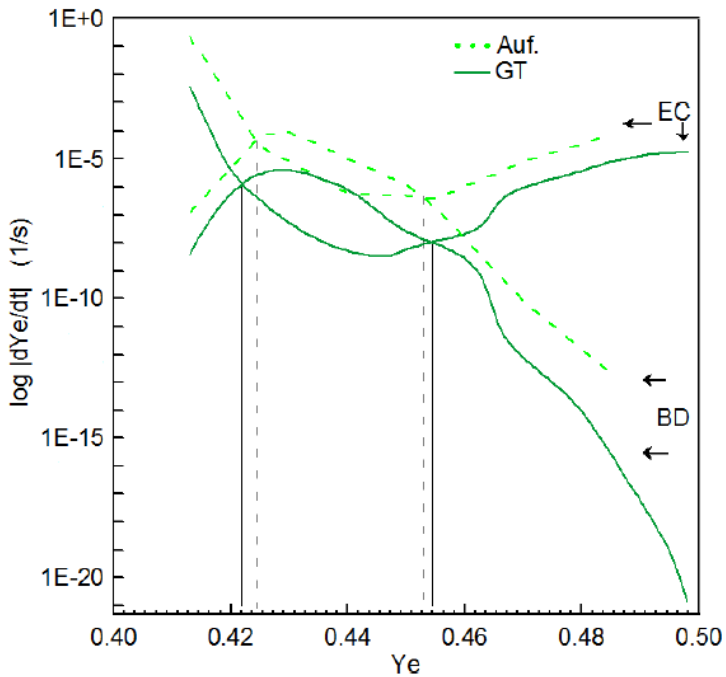

Fig. 11.— Temporal derivative $\dot{Y}_e$.

$$\frac{dY_e}{dt} = \frac{dY_e^{EC}}{dt} + \frac{dY_e^{\beta}}{dt}, = \sum_k \frac{X_k}{A_k}(-\lambda_k^{EC} + \lambda_k^{\beta}),$$

The increment of this interval could have important consequences over the core collapse, since it can to keep the equilibrium of the stellar nucleus for more time, retarding reduction of the degeneration pressure, and then consequently the collapse. Thus, a slow collapse could reduce the velocity of density increase, and consequently could reduce the pressure, which is in opposition to the initial core contraction.

R.C. Ferreira, A. J. Dimarco and A. R. Samana, C. Barbero, submetido a Astrophys. Journal.
R. C Ferreira Master Thesis- PROFISICA

Summary: on weak-nuclear interaction

- All the formalism to describe weak-nuclear interaction present in the literature are equivalents!

(i)O'Connell, Donelly & Walecka, PR6,719 (1972)
seven irreducible tensor operators (ITO) separated in longitudinal, coulomb, transversal electric, transversal magnetic used in electro Scattering (T. deforest and J.D. Walecka, Adv. in Phys. 15 (1966) 1)

(ii) Kuramoto etal. NPA 512, 711 (1990), up to $(|k|/M)^3$ in the weak hamiltonian.

(iii) Luyten etal. NP41,236 (1963), developed to evaluate muon capture

(iv) Krmpotic etal. PRC71, 044319(2005), using a notation more familiar to the beta decay working with allowed, 1F, 2F, etc transitions.

Summary: on nuclear models

QRPA-type Models

disadvantages:
Low energy neutrino regions up to 250 MeV,
Skyrme interaction not good enough to
make decisive improvement,
Gogny interaction to check Skyrme, spherical nuclei, few QRPA model to non-spherical nuclei
advantages:
self-consistency, large space, excellent agreement with exclusive reaction as well as SM, well description inclusive reaction and it´s possible describe up to 600 MeV neutrino energy with RQRPA, good option for astrophysical systematic calculations , main tool for 2 beta decay in the last 30 years
improvements:
through the Universal Nuclear Density Functional –UNEDF, non-spherical nuclei,

Global Models(GTBD)

disadvantages:
not well description of ground state properties.
non-microscopic
advantages:
statistical, work easily with many nuclei
improvements:
use new one-particle strength functions.

Large Scale Shell Model

disadvantages:
only magic nuclei (N=50, 82, 126);
only GT-decay;
only spherical, great computational
task, some cut due to configurational space
could be dangerous
advantages:
several essential correlations included;
treatment of even-even and odd
isotopes.
improvements: Ab-initio shell model, new advances in nuclei as 12C,16O and 48Ca

P. Möller
"…there is no "**correct**" model in nuclear physics. Any modeling of nuclear-structure properties involves approximations … to obtain a formulation that can be solved…, but that "**retains the essential features**" of the true system."